

# THE ORIGIN OF BINARY STARS

---

Joel E. Tohline

*Department of Physics and Astronomy, Louisiana State University, Baton Rouge, Louisiana 70803; email: tohline@rouge.phys.lsu.edu*

**Key Words** star formation, binaries

■ **Abstract** Although we have a general understanding of the manner in which individual stars form, our understanding of how binary stars form is far from complete. This is in large part due to the fact that the star formation process happens very quickly and in regions of the Galaxy that are difficult to study observationally. We review the theoretical models that have been developed in an effort to explain how binaries form. Several proposed mechanisms appear to be quite promising, but none is completely satisfactory.

## INTRODUCTION

This review of the ideas that have been put forward to explain the origin of binary stars builds upon a foundation that has been laid by two earlier articles in this Annual Review series: The first, published 15 years ago by Shu, Adams & Lizano (1987), focused on a discussion of the origin of single stars; the second, published 8 years ago by Mathieu (1994), reviewed the observational evidence of binary systems in the pre-main-sequence (PMS) stellar population. Because the ideas presented in these two earlier reviews are essential ingredients to any discussion of the origin of binary stars, I spend a bit of time recapitulating them, but lack of space requires me to refer the reader to these articles for details. The task of reviewing this topic has been considerably simplified because of the conference that was held in April, 2000, on the topic of “The Formation of Binary Stars” (Zinnecker & Mathieu 2001).

## Background

Shu et al. (1987) have provided the following outline of the various stages of the birth of single stars. The process begins with a molecular cloud, after its basic constituent material has been assembled somehow and somewhere in a galaxy. The cloud is gravitationally bound, but as a whole it is supported against gravitational collapse by the presence of a magnetic field. Stage I: Via ambipolar diffusion, the magnetic field slowly leaks out of relatively over-dense regions of the cloud, allowing these regions to become more and more dense, relative to their surroundings.

In this way, observationally identifiable “molecular cloud cores” are formed. Stage II: The star formation process begins in earnest when a condensing cloud core “passes the brink of instability” (Shu et al. 1987) and collapses dynamically toward stellar densities. This leads to the formation of a central protostar embedded within an infalling envelope of dust and gas. A disk almost always surrounds the embedded protostar, reflecting the fact that molecular cloud cores are almost always rotating. The protostar accretes matter, largely from the infalling cloud in which it is embedded, but to some degree also from its surrounding disk. As it contracts toward the main sequence, the protostar develops a stellar wind, which initially is unobservable because “the ram pressure from material falling directly onto the [proto]stellar surface suppresses breakout” (Shu et al. 1987). Stage III: Gradually, direct infall onto the protostar’s surface weakens as incoming material with relatively high specific angular momentum falls preferentially onto the disk. The stellar wind is then able to break out in the direction of the system’s rotational poles, creating an observable bipolar flow. Stage IV: The amount of material added to the protostar via direct infall continues to decrease, and the opening angle of the wind steadily widens until the young central star (along with its surrounding nebular disk) is revealed as a bonafide PMS star—for example, a T Tauri star. Stage V: Over time, the nebular disk finally disappears.

As Mathieu (1994) has reviewed, it is clear from an observational perspective that the PMS stellar population is rich in multiple systems. The overall frequency of occurrence of binary stars among the PMS population is at least as large as has been documented for main-sequence stars (Duquennoy & Mayor 1991), that is, certainly greater than 50%. Young, stellar-mass binary systems have been found with semimajor axes ranging from 0.02 to  $10^3$  AU (orbital periods ranging from a couple of days to  $10^4$  years), with a binary frequency distribution as a function of semimajor axis that is qualitatively consistent with the log-normal-like distribution found for main-sequence stars. With this evidence in hand, Mathieu (1994) concluded that “binary formation is the *primary* branch of the star-formation process.” Also, it seems clear that the process (or processes) responsible for creating binary stars generally exerts its influence before stage IV. These realizations have led to an increased effort over the past decade to understand from a theoretical perspective how binary star systems form.

In the eight years since Mathieu compiled his review, significant advances have been made in the techniques and instrumentation that are available to identify and study binary stars that have a wide range of orbital periods, mass ratios, and ages. These include HST (WFPC2 & NICMOS) imaging (Padgett et al. 1997, 1999; Reid et al. 2001), submillimeter imaging (Smith et al. 2000), optical and infrared long-baseline interferometry (Quirrenback 2001a,b), millimeter and submillimeter interferometry (Launhardt et al. 2000, Launhardt 2001, Guilloteau 2001), adaptive optics (Simon et al. 1999, Close 2001), Hipparcos astrometric observations (Söderhjelm 1999; Quist & Lindgren 2000, 2001), and microlensing (Alcock et al. 2001, Di Stefano 2001). A fair fraction of the increased observational activity in this arena certainly has been stimulated by the discovery

of extrasolar planetary systems (Mayor & Queloz 1995; Marcy & Butler 1998, 2000). Although all of this work is important in establishing a database that can, in the long run, be used to critically evaluate theoretical models proposed to explain how binary (and other multiple) star systems form, it is fair to say that, at present, our understanding of process(es) by which binary systems form is far too crude to take full advantage of the detailed information that is housed in such a database. For the purpose of this review, it is sufficient to build our discussion on the two broad conclusions drawn by Mathieu (1994): Stars preferentially form in pairs, and binary formation occurs prior to the PMS phase of a star's evolution.

## Basic Physical Principles

Throughout this review, there is very little discussion of the role that magnetic fields play in the star formation process. This stands in stark contrast to the earlier review by Shu et al. (1987). The reasons for downplaying the role of magnetic fields here are twofold. First, although there is a considerable body of evidence [see the discussion by Shu et al. (1987)] supporting the conclusion that the interstellar magnetic field significantly influences the onset of gravitational collapse in molecular clouds, the general consensus is that the field will largely decouple from a contracting cloud at number densities  $\gtrsim 10^{10} \text{ cm}^{-3}$  because, at such high densities, the fractional ionization of the gas becomes extraordinarily small. Because, as is emphasized below, the processes likely to be responsible for transforming single gas clouds into binary protostellar systems largely operate at densities higher than this limit, neglect of the magnetic field is justified. Second—and largely justified by the first—researchers who have focused their modeling efforts on the binary star formation problem generally have ignored the effects of magnetic fields, so a review of this body of work must naturally downplay the influence of magnetic fields as well. We return to the issue of the influence that magnetic fields have on the onset of collapse in “Summary and Conclusions,” below.

By ignoring the effects of magnetic fields, we in practice (although not in spirit) depart somewhat from the storyline presented by Shu et al. (1987) and summarized above. Specifically, when the text of the earlier review refers to a cloud core that has “passed the brink of instability” and thereby entered stage II of the star formation process, it is referring to a critical physical condition in the cloud core that is established, in part, by the strength of the cloud's magnetic field. We instead use this phrase to refer to the classic thermal Jeans instability (see the relevant definition in “The Jeans Instability,” below). Even in the case in which the effects of magnetic fields are considered, of course, the Jeans instability is relevant, but it may establish only a necessary rather than sufficient condition for collapse.

**PHYSICAL PARAMETERS** We characterize a protostellar gas cloud or protostar by its total mass  $M$  and radius  $R$ , its mean temperature  $T$  and mean molecular weight

$\mu$ , and its mean angular velocity  $\omega$ . From  $M$ ,  $R$ , and  $\mu$  we can determine the cloud's mean mass density,

$$\bar{\rho} \equiv \frac{3M}{4\pi R^3}, \quad (1)$$

and its corresponding number density,

$$n = \frac{\bar{\rho}}{\mu m_p}, \quad (2)$$

where  $m_p$  is the mass of a proton. We also specify that, upon compression, the cloud's temperature varies with its density as

$$T \propto \bar{\rho}^{\gamma-1}, \quad (3)$$

where  $\gamma$  is the effective adiabatic exponent of the gas. It is understood that  $\gamma$  itself is likely to be a function of the cloud's density (see the discussion below in association with Figure 2). From  $T/\mu$  and  $\gamma$ , the mean sound speed of the gas can be determined via the expression,

$$c_s = \left[ \gamma \frac{\Re T}{\mu} \right]^{1/2}, \quad (4)$$

where  $\Re$  is the gas constant.

As Shu et al. (1987) have reminded us, star formation is a complex process that spans many orders of magnitude in mass and linear scale. If, following Shu et al., we concentrate on aspects of the problem that occur on scales ranging from that of a giant molecular cloud to the shortest period PMS binaries (e.g., Table A2 of Mathieu 1994), then we have to deal with systems having masses in the range of  $10^6 \gtrsim M/M_\odot \gtrsim 1$  and linear scales in the range of  $10^{20} \text{ cm} \gtrsim l \gtrsim 10^{12} \text{ cm}$  (that is,  $30 \text{ pc} \gtrsim l \gtrsim 10 R_\odot$ ). The bottom diagram in Figure 1 illustrates this range of length scales, with the letters *GMC* drawn on the left to mark the size of a giant molecular cloud and the letter *B* drawn near the right to mark the scale (orbital separation) of a PMS binary star with an orbital period of only a couple of days. The letter *P* in this diagram marks the linear scale of our own planetary system (40 AU, as set by the orbit of Pluto), which lies between the two extremes. Rotationally flattened disks of this size or larger are now almost always found in association with the youngest binary or single PMS stars. As a point of reference, the top diagram in Figure 1 illustrates that a comparable range of length scales takes us from the present scale of the universe (marked by *U* on the diagram), through the size of a typical galaxy (marked by *G*), to the size of a typical globular cluster (marked by *GC*). This comparison of scales serves to emphasize the complexity of the problem at hand. That is, we should not be surprised to find that the process by which binary stars form from molecular clouds in our Galaxy is at least as difficult to understand and to model uniquely as the process by which globular clusters form from an homogeneous and isotropic universe.

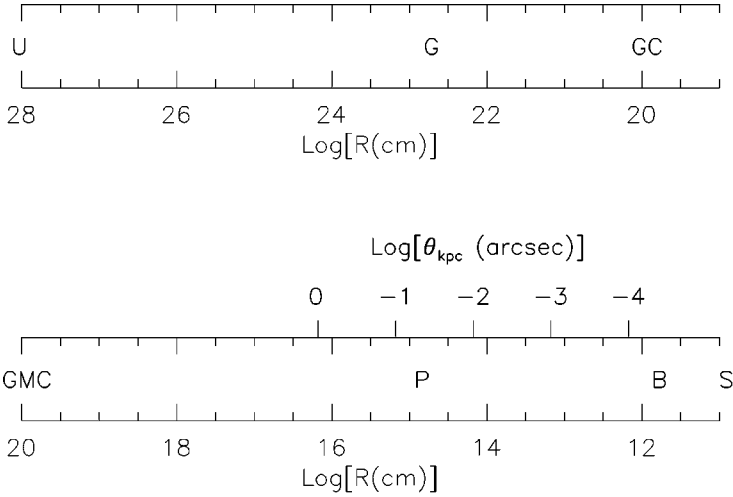


**Figure 1** Two scales that, together, cover over 40 orders of magnitude in length. They stretch from the scale of the universe (*U* at the left-hand edge of top scale), through our Galaxy (*G*) to the scale of an individual globular cluster (*GC*); and from the scale of a giant molecular cloud (*GMC*), through our planetary system (*P*) down to the scale of the shortest period pre-main-sequence binaries (*B*) and the radius of the Sun (*S*). Along the bottom scale we have also indicated the angular resolution  $\theta_{\text{kpc}}$  (in arcsec) that is required to resolve a system of radius  $R$  at a distance of 1 kpc. Notice that there is roughly the same separation between the scale of the universe and the size of individual GCs as there is between the scale of a GMC and the shortest period binary systems.

At a distance  $d_{\text{kpc}}$  (measured in kiloparsecs) from the solar system, an object of linear scale  $R_{\text{AU}}$  (measured in astronomical units) will subtend an angle  $\theta_{\text{kpc}}$  (measured in seconds of arc) given by the expression,

$$\theta_{\text{kpc}} = 10^{-3} \frac{R_{\text{AU}}}{d_{\text{kpc}}}. \quad (5)$$

Hence, as the top scale in the bottom diagram of Figure 1 indicates, at a distance of 1 kpc a 40-AU disk will subtend an angle  $\theta_{\text{kpc}}$  of 40 milli-arcseconds on the sky; at this same distance a resolution of a tenth of a milli-arcsecond or better would be required to spatially resolve the shortest period PMS binaries.

Figure 2 illustrates the range of densities and temperatures that a stellar-mass gas cloud must traverse as it contracts from a molecular cloud state toward a structure (on the zero-age main sequence) that is hot enough and dense enough to fuse hydrogen. For purposes of illustration, the solid curve identifies the approximate  $\rho - T$  path that is expected to be followed by the central-most region of a nonrotating (spherically symmetric) protostellar cloud containing a total mass  $M \sim 1-3 M_{\odot}$  (drawn from Figure 3 of Tohline 1982 and Figure 27.3 of Kippenhahn & Weigert

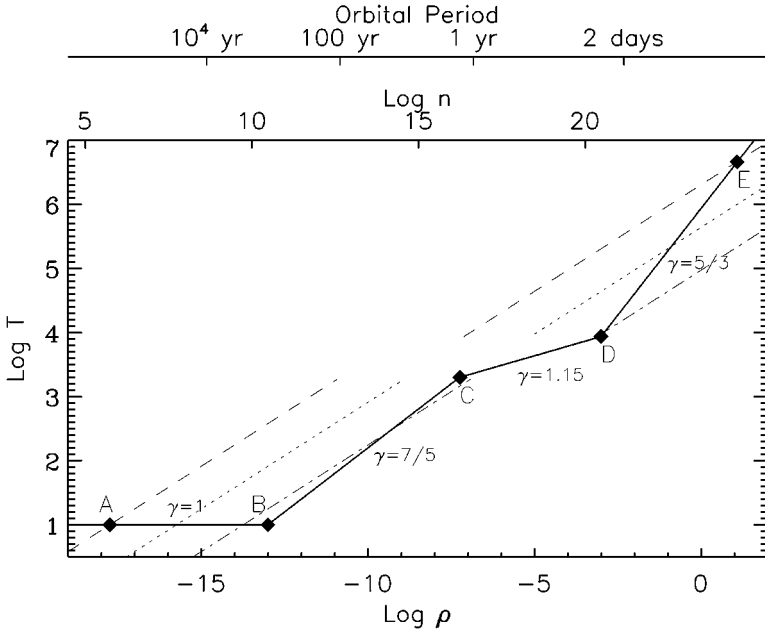


**Figure 2** The evolutionary trajectory (*solid curve*) of the central region of a proto-stellar gas cloud is shown in the temperature-density plane. (Patterned after Figure 3 of Tohline 1982.) The slope of each segment of the curve is indicated by the value of the effective adiabatic exponent  $\gamma$ , as defined in Equation 3. The density is shown both in  $\text{g cm}^{-3}$  (*bottom horizontal axis*) and in  $\text{cm}^{-3}$  (*top horizontal axis*); the temperature is given in degrees Kelvin. Also shown along the top of the plot is the orbital period of a binary system that has the equivalent mean density, as determined through Equations 10 and 6. For reference, lines of constant  $M_{\text{equil}}$ , as defined by Equation 22, have been drawn at values of  $1 M_{\odot}$  (*dashed*),  $10^{-1} M_{\odot}$  (*dotted*), and  $10^{-2} M_{\odot}$  (*dash-dot*); the vertical gap between temperatures of 2,000 K and 10,000 K signifies that the molecular gas is being dissociated and ionized; hence,  $\mu$  changes from 2 (*lower section of each line*) to 1/2 (*upper section of each line*).

1990; see also Figure 2 of Winkler & Newman 1980, Figure 3 of Boss 1984, and Figure 1 of Bate 1998). Various segments of this curve have been labeled with the value of the effective adiabatic exponent  $\gamma$  that governs the illustrated  $\rho - T$  relationship, as defined above by Equation 3.

**KEY TIMESCALES** From  $\bar{\rho}$ ,  $c_s$ ,  $\omega$ , and  $R$ , we can derive three key timescales: The free-fall time,

$$\tau_{\text{ff}} = \left[ \frac{3\pi}{32G\bar{\rho}} \right]^{1/2}, \tag{6}$$

where,  $G$  is the gravitational constant; the sound-crossing time,

$$\tau_s = \frac{R}{c_s}; \quad (7)$$

and the rotation period of the cloud,

$$\tau_{\text{rot}} = \frac{2\pi}{\omega}. \quad (8)$$

When discussing binary star (or binary protostellar) systems, a fourth relevant timescale is the binary's orbital period,

$$P = \left[ \frac{4\pi^2 a^3}{GM_{\text{tot}}} \right]^{1/2}, \quad (9)$$

where  $M_{\text{tot}}$  is the total mass of the system, and  $a$  is the system's semimajor axis [for circular orbits,  $a$  is the distance between the two stars (or protostars)]. Notice, however, that the orbital period is not much different from the free-fall time, in the following sense. If a gas cloud of radius  $R$  and mass  $M$  is transformed (by some, as yet, unspecified mechanism) into a binary star system of mass  $M_{\text{tot}} = M$  and separation  $a = R$ , then by Equations 9 and 6 the binary will have an orbital period,

$$P = 32^{1/2} \tau_{\text{ff}} \approx 5.7 \tau_{\text{ff}}. \quad (10)$$

Because, as shown by Equation 6, the free-fall time of a gas cloud (or protostar) depends only on the cloud's mean mass density, Equation 10 suggests that the measured orbital period of a binary system tells us something directly about the density of the gas cloud from which the binary system formed. With this in mind, the top horizontal axis in Figure 2 has been labeled with the binary orbital period that corresponds to the mean mass density that is given along the bottom horizontal axis of the figure.

Also by way of illustration, Table 1 lists the values of some relevant physical parameters at a variety of different scales that should be of interest to researchers

**TABLE 1** Scales of interest

$P_{\text{orbit}}$ [years]	$n_{\text{H}_2}$ [ $\text{cm}^{-3}$ ]	$\Delta v / \Delta \theta_{\text{kpc}}$ [ $\text{km s}^{-1}/\text{arcsec}$ ]	$a$ [AU] for $1 M_{\odot}$
380000	$3 \times 10^5$	0.04	5200
20000	$1 \times 10^8$	0.75	740
3800	$3 \times 10^9$	3.7	250
1000	$4 \times 10^{10}$	15.	100
300	$5 \times 10^{11}$	50.	45
100	$4 \times 10^{12}$	150.	20

searching for evidence of protostellar binary systems in molecular clouds. For example, a binary system that forms from an environment in which the mean cloud density  $n_{\text{H}_2} \sim 3 \times 10^5 \text{ cm}^{-3}$  should have an orbital period  $P \sim 4 \times 10^5$  years and should exhibit a velocity gradient on the sky  $\Delta v / \Delta \theta_{\text{kpc}} \sim 0.04 \text{ km s}^{-1}/\text{arcsec}$  [e.g., the properties of the Bok Globule CB230 described by Launhardt et al. (2000)]. If this system contains  $1 M_{\odot}$  of material, the separation of its binary components will be  $\sim 5200 \text{ AU}$ , which at a distance of  $1 \text{ kpc}$  will subtend an angle of  $\theta_{\text{kpc}} \sim 5.2 \text{ arcsec}$ . A bound system with an orbital period of  $\sim 1000$  years, however, must form in an environment that has a much higher mean density,  $n_{\text{H}_2} \sim 4 \times 10^{10} \text{ cm}^{-3}$ . It should exhibit a significantly higher velocity gradient on the sky,  $\Delta v / \Delta \theta_{\text{kpc}} \sim 15 \text{ km s}^{-1}/\text{arcsec}$ , but will subtend a much smaller angle on the sky: At  $1 \text{ kpc}$ , a  $1 M_{\odot}$  system should have  $\theta_{\text{kpc}} \sim 0.1 \text{ arcsec}$ .

Finally, we should mention the accretion timescale,

$$\tau_{\text{accrete}} = \frac{m_0}{\dot{M}}, \quad (11)$$

which gives the time that it takes an equilibrium structure (e.g., the central core of a collapsing cloud) of mass  $m_0$  to double in mass as it accretes material from a surrounding cloud or disk at a rate  $\dot{M}$ . Over intervals of time that are short compared to  $\tau_{\text{accrete}}$ , the mass of the central structure remains relatively unchanged, so the central structure can be considered dynamically isolated from its surroundings. The accretion rate  $\dot{M}$  varies from situation to situation, but in discussions of the free-fall collapse of protostellar gas clouds, two rates are of particular interest. The first comes simply from the ratio of a cloud's total mass to its initial free-fall time,

$$\dot{M}_{\text{ff}} = \frac{M}{\tau_{\text{ff}}}. \quad (12)$$

The second is the accretion rate  $\dot{M}_{\text{sis}}$  highlighted by Shu (1977) that arises from the collapse of the so-called singular isothermal sphere,

$$\dot{M}_{\text{sis}} = \frac{c_s^3}{G}. \quad (13)$$

**IMPLICATIONS OF THE VIRIAL THEOREM** From  $M$  and  $R$  we obtain the following estimate of the configuration's total gravitational potential energy,

$$E_{\text{grav}} \sim -\frac{3}{5} \frac{GM^2}{R}. \quad (14)$$

From  $M$  and  $T/\mu$  we obtain an estimate of its total thermal energy via the expression,

$$E_{\text{therm}} \sim \frac{3}{2} \frac{\mathfrak{R}}{\mu} MT. \quad (15)$$



The configuration's rotational kinetic energy is

$$E_{\text{rot}} = \frac{1}{2} I \omega^2 = \frac{1}{2} \frac{J^2}{I} \sim \frac{1}{5} M R^2 \omega^2, \quad (16)$$

where  $I \approx \frac{2}{5} M R^2$  is the configuration's principal moment of inertia and  $J = I \omega$  is its total angular momentum. From the virial theorem (e.g., Hansen & Kawaler 1994), we know that the following relationship between these three global energy reservoirs must hold if a protostellar gas cloud (or protostar) is in equilibrium:

$$2(E_{\text{therm}} + E_{\text{rot}}) + E_{\text{grav}} = 0 \quad (17)$$

or

$$\alpha + \beta = \frac{1}{2}, \quad (18)$$

where

$$\alpha \equiv \frac{E_{\text{therm}}}{|E_{\text{grav}}|} \sim \frac{5}{2} \frac{\mathfrak{N}}{\mu} T \frac{R}{GM}, \quad (19)$$

$$\beta \equiv \frac{E_{\text{rot}}}{|E_{\text{grav}}|} \sim \frac{1}{3} \frac{R^3 \omega^2}{GM}. \quad (20)$$

If a cloud (or protostar) is in equilibrium but is not rapidly rotating ( $\beta \ll 1/2$ ), according to Equations 18 and 19,  $\alpha \approx 1/2$  and its mass must be related to its radius and mean temperature via the expression

$$M_{\text{equil}} \sim 5 \frac{\mathfrak{N}}{\mu} T \frac{R}{G}. \quad (21)$$

Using Equation 1, we can alternatively express this equilibrium mass in terms of the cloud's mean density and temperature as follows:

$$M_{\text{equil}} \sim 5.5 \left[ \frac{\mathfrak{N} T}{\mu G} \right]^{3/2} \bar{\rho}^{-1/2}. \quad (22)$$

For reference, lines of constant  $M_{\text{equil}}$  have been drawn in Figure 2 at values of  $1 M_{\odot}$  (*dashed*),  $10^{-1} M_{\odot}$  (*dotted*), and  $10^{-2} M_{\odot}$  (*dash-dot*); the vertical gap between temperatures of  $2000^{\circ}\text{K}$  and  $10,000^{\circ}\text{K}$  signifies that the molecular gas is being dissociated and ionized, hence  $\mu$  changes from 2 (lower section of each line) to  $1/2$  (upper section of each line). (The lines have a slope of  $1/3$  in this log-log plot.) Combining Equation 21 with Equations 1, 4, 6, and 7, this statement of equilibrium also means that the sound-crossing time and the free-fall time are approximately equal to one another in the cloud (or protostar), that is,

$$\tau_s \approx \tau_{\text{ff}}. \quad (23)$$

On the other hand, if a cloud's equilibrium state is balanced against gravity largely by rotation ( $\alpha \ll 1/2$  and  $\beta \approx 1/2$ ), then the virial theorem states that the

cloud’s mean angular velocity will be near its maximum allowable value,

$$\omega \approx \omega_{\max} \approx [2\pi G \bar{\rho}]^{1/2}; \tag{24}$$

that is, the cloud’s rotation period will be

$$\tau_{\text{rot}} = \frac{2\pi}{\omega} \approx 4.6\tau_{\text{ff}}. \tag{25}$$

Not surprisingly, this is essentially equal to the orbital period of a binary system that has a separation  $a = R$  and the same total mass, as discussed above in connection with Equation 10.

**THE JEANS INSTABILITY** If, for a given  $M, R, T/\mu$ , and  $\omega$ , one finds that  $\alpha + \beta < 1/2$  in a protostellar gas cloud, then the cloud will collapse on a free-fall timescale. In the absence of rotation, this condition ( $\alpha < 1/2$ ) is simply a statement that

$$M > M_{\text{equil}} \tag{26}$$

and, hence, that the cloud has encountered the classic Jeans instability (Jeans 1919). In this context, Equations 21 and 22 given above for  $M_{\text{equil}}$  also serve to define the familiar Jeans mass,  $M_J$ ; that is to say,

$$M_J \sim 5 \frac{\mathfrak{R}}{\mu} T \frac{R}{G} \sim 5.5 \left[ \frac{\mathfrak{R}}{\mu} \frac{T}{G} \right]^{3/2} \bar{\rho}^{-1/2}. \tag{27}$$

When the mass of a molecular cloud or cloud core exceeds this critical mass, it has “passed the brink of instability” and entered stage II of the star formation process (Shu et al. 1987. For example, at 10°K a uniform-density, 1  $M_{\odot}$  molecular gas cloud will encounter this Jeans instability at the point marked A in Figure 2 ( $\bar{\rho} = 1.8 \times 10^{-18}$  g cm<sup>-3</sup>) (see Table 2). As it collapses, it will evolve (to the right in Figure 2) to configurations of higher density and smaller radius.

**TABLE 2** Typical conditions in collapsing cloud core (see Figure 2)

Case	$\rho$ [g/cm <sup>3</sup> ]	$T$ [°K]	$\gamma$	$\mu$	$\frac{1}{\gamma} c_s^2$ [cm <sup>2</sup> /s <sup>2</sup> ]	$M_{\text{equil}}$ [ $M_{\odot}$ ]	$j_{\text{max}}$ [cm <sup>2</sup> /s]
A	$1.8 \times 10^{-18}$	10	1	2	$4.2 \times 10^8$	1	$3.6 \times 10^{21}$
B	$1.0 \times 10^{-13}$	10	$\frac{7}{5}$	2	$4.2 \times 10^8$	0.004	$1.5 \times 10^{19}$
C	$5.7 \times 10^{-8}$	2000	1.15	1	$1.7 \times 10^{11}$	0.05	$8.3 \times 10^{18}$
D	$1.0 \times 10^{-3}$	$8.7 \times 10^3$	$\frac{5}{3}$	$\frac{1}{2}$	$1.4 \times 10^{12}$	0.008	$5.1 \times 10^{17}$
E	$1.2 \times 10^1$	$4.6 \times 10^6$	$\frac{5}{3}$	$\frac{1}{2}$	$7.7 \times 10^{14}$	1	$2.6 \times 10^{18}$

Notice that the mass of a cloud can be expressed very simply in terms of the Jeans mass and the dimensionless energy parameter  $\alpha$  as follows:

$$M = \frac{M_J}{2\alpha}. \quad (28)$$

Therefore, if a protostellar gas cloud collapses from a state in which  $\alpha$  is only slightly less than  $1/2$ , that is equivalent to saying that the cloud's mass is only slightly greater than one Jeans mass initially. In this case, one can show (see, for example, the discussion associated with Equation 23 of Shu et al. 1987) that the relevant accretion timescale  $\tau_{\text{accrete}}$  can be derived from the accretion rate defined by either Equation 12 or 13. That is to say, the model of a collapsing singular isothermal sphere is relevant (Larson 1969, Penston 1969, Shu 1977) and  $\dot{M}_{\text{ff}} \approx \dot{M}_{\text{sis}}$ . If, however,  $\alpha \ll 1/2$  initially, then the cloud initially encloses many Jeans masses and is well past the brink of instability. (One might fairly ask how the cloud was brought to such a drastic state in the first place. See "Summary and Conclusions," below.) In this case, the singular isothermal sphere solution becomes irrelevant and the appropriate accretion timescale must be estimated from Equation 12.

**THE IMPORTANCE OF THE EFFECTIVE ADIABATIC EXPONENT  $\gamma$**  Once a cloud encounters the Jeans instability, it will evolve dynamically until it acquires a new configuration in which virial equilibrium is achieved, that is, until the sum  $(\alpha + \beta)$  climbs up to the value  $1/2$ . We can therefore estimate how far a given cloud will collapse before it settles into an equilibrium state by examining how the two energy ratios  $\alpha$  and  $\beta$  scale with the cloud's radius or mean density. Assuming that the cloud's mass  $M$  and angular momentum  $J$  are conserved during its dynamical collapse, Equations 1, 16, and 20 give

$$\beta \propto R^{-1} \propto \bar{\rho}^{1/3}, \quad (29)$$

and Equations 3 and 19 give,

$$\alpha \propto TR \propto \bar{\rho}^{\gamma-4/3}. \quad (30)$$

Equation 30 identifies the critically important role that the effective adiabatic exponent plays in star formation. According to this expression, if  $\gamma < 4/3$ , the energy ratio  $\alpha$  actually decreases during a collapse. Therefore it is impossible for thermal pressure alone to stop the cloud's free-fall collapse as long as the cloud evolves through a density-temperature regime where the effective adiabatic exponent  $\gamma < 4/3$ , such as the isothermal ( $\gamma = 1$ ) regime illustrated in the left-hand portion of Figure 2. This is why in models of spherically symmetric collapse (e.g., Larson 1969, Winkler & Newman 1980) the cloud's free-fall is not slowed until its central-most region reaches a density  $\sim 10^{-13} \text{ g cm}^{-3}$  (the point marked *B* in Figure 2) and starts to become opaque to the cloud's primary cooling radiation. Quoting directly from Larson (1969), "... the heat generated by the collapse in this region is then no longer freely radiated away, and the compression becomes

approximately adiabatic” with an effective adiabatic exponent ( $\gamma \approx 7/5$ ) that is greater than  $4/3$ .

Thus, in a spherically symmetric cloud, a minimum of two conditions must be met before a stable equilibrium configuration can be achieved:  $\alpha = 1/2$ , that is,  $M = M_{\text{equil}}$ ; and  $\gamma > 4/3$ . In Figure 2, the segments of the (*solid*) evolutionary track for which a stable equilibrium is possible are the segments for which  $\gamma > 4/3$ . On each of these segments the mass required to achieve an equilibrium ( $\alpha = 1/2$ ) is given by the value of the (*dashed, dotted, or dash-dot*)  $M_{\text{equil}}$  line that intersects the evolutionary track. For example, at the point marked *B* in Figure 2, equilibrium will be achieved with a mass  $\sim 4 \times 10^{-3} M_{\odot}$ . This is why the first core that forms in the collapse models of Larson (1969) and Winkler & Newman (1980) contains only a very small fraction of the cloud’s total mass—only a few Jupiter masses!

Notice that a spherically symmetric cloud that contains an entire solar mass of material can achieve virial equilibrium in only two places along the evolutionary track shown in Figure 2: at the point marked *A* [at a very low density and temperature ( $\bar{\rho} \sim 1.8 \times 10^{-18} \text{ g cm}^{-3}$ ,  $T \sim 10 \text{ K}$ )] or at the point marked *E* [at a very high density and temperature ( $\bar{\rho} \sim 12 \text{ g cm}^{-3}$ ,  $T \sim 5 \times 10^6 \text{ K}$ )]. The only stable configuration is the high-density one because it resides on a portion of the evolutionary track for which  $\gamma > 4/3$ . Thus, once the Jeans instability is encountered (at point *A*), the dynamical collapse must proceed on a free-fall timescale—through almost 19 orders of magnitude in density—to a star-like configuration. A central, low-mass core will form along the way (as in the models of Larson 1969 and Winkler & Newman 1980) only if the collapse proceeds in a nonhomologous fashion (see “Nonhomologous Collapses,” below).

The free-fall collapse of a rotating cloud can be halted at much lower densities because, as shown by Equation 29,  $\beta$  always increases as the cloud contracts. Hence, even during the isothermal phase of a cloud’s contraction, virial balance can be achieved when  $\beta$  grows to a value of  $(1/2 - \alpha)$ . Hence, there will be a tendency for  $\beta$  to climb up to a value  $\sim 1/2$  during the phase of isothermal contraction because, for the cloud as a whole,  $\alpha$  will drop to a very small value.

Once again, though, virial equilibrium alone does not guarantee a configuration that is stable against further collapse. As in the nonrotating case just described, an additional condition involving the effective adiabatic exponent must be met for stability. According to the detailed stability analysis of nearly spherical systems presented by Ledoux (1945; see also the discussion associated with Figure 3 in Tohline 1984), the condition for stability is,

$$\gamma > \gamma_{\text{crit}} \approx \frac{2(2 - 5\beta)}{3(1 - 2\beta)}. \quad (31)$$

When  $\beta \rightarrow 0$ , this expression produces the value of  $\gamma_{\text{crit}} = 4/3$  that is familiar for spherically symmetric, nonrotating gas clouds. When  $\beta \neq 0$ , this expression shows that  $\gamma_{\text{crit}}$  is somewhat less than  $4/3$ . However, according to Equation 31, a rotating, isothermal ( $\gamma_{\text{crit}} = 1$ ) gas will not be stable against further radial collapse unless  $\beta > 1/4$ . Complementary analyses of equilibrium structures by Hayashi

et al. (1982), Tohline (1984), and Hachisu & Eriguchi (1985) have confirmed that rotationally flattened, axisymmetric, isothermal gas clouds are stable against dynamical collapse (or expansion) only if  $\beta \gtrsim 0.25\text{--}0.3$ .

## Possible Formation Mechanisms

The mechanisms proposed for forming binary stars can be divided into three broad categories. First, it is possible that Jeans-unstable gas clouds preferentially collapse to form single stars; then, after formation, the stars become bound together in pairs via a process usually referred to as “capture.” Second, either during or immediately after its free-fall collapse, an individual rotating gas cloud may spontaneously break into two pieces that are in orbit about one another. In this process, which we refer to as “prompt fragmentation,” the cloud’s original spin angular momentum is converted fairly directly into orbital angular momentum of the binary system. Third, the central-most regions of a rotating gas cloud may collapse to form an equilibrium configuration that is initially stable against fragmentation. Then, as this relatively dense core contracts toward the main sequence while accreting relatively high specific angular momentum material from the outer regions of the cloud, the core (or its surrounding accretion disk) may encounter an instability that leads to the formation of a binary system. We refer to this process as “delayed breakup.”

## CAPTURE

It is possible that binary stars form by the relatively simple mechanism of capture. That is to say, it is possible that stars preferentially form as single objects along the lines described by Shu et al. (1987), then after formation become grouped together in bound pairs through dynamical encounters. As Clarke (1992) has reviewed, though, the formation of a binary from two initially unbound stars requires the dissipation of some fraction of the energy of their relative orbit. In favorable three-body encounters, the energy lost from the relative orbit of the two stars can be transferred as kinetic energy to a third star. Although rare, such encounters can significantly influence the evolution of the central-most regions of globular star clusters (e.g., Portegies et al. 1997). But this cannot be the mechanism responsible for the formation of most binary systems in large clusters or in the field because the frequency of such favorable encounters is extremely low. Also, in large virialized clusters, the typical velocity of approach of unpaired stars is unfavorably hyperbolic. Whereas this is less of a problem in smaller N-body systems, simulations show that purely gravitational encounters yield relatively few binaries per cluster, and these binaries tend to form from the most massive stellar components of a cluster (Clarke 1992, Valtonen & Mikkola 1991).

Two-body encounters can result in the formation of a binary system from an initially unbound pair if the interaction is not purely gravitational. For example, orbital energy can be converted into heat through the excitation of tides in one or both stars. However, significant tides are raised only during very close encounters—which

require relatively special initial conditions—and in the absence of strong tides many encounters are required to dissipate a significant amount of energy. Hence, this traditional tidal capture mechanism is unlikely to explain how young, PMS binaries are formed. In protostellar environments, however, the material that resides in the extended disks around young stars (or protostars) can also be tidally disturbed during an encounter and thereby absorb a portion of the orbital energy. Larson (1990) estimated that a large fraction of all stars might be incorporated into binaries through this mechanism during the PMS phase. Subsequent detailed investigations have shown, however, that even when disks are included to enhance the cross-section for collisions, tidal capture still does not work effectively enough. Typically the velocities of encounter are sufficiently large that they disrupt the disk (Clarke & Pringle 1993). It appears, therefore, that in all but the smallest virialized clusters, star-disk capture cannot be responsible for the formation of most binaries.

## PROMPT FRAGMENTATION

Prompt fragmentation is the binary formation process that has received by far the most attention over the past two decades. This is in large part due to the relative capabilities and limitations of the numerical tools that have been employed to study binary star formation. Binary fragmentation is, by definition, a nonlinear process that exhibits no simple geometric symmetries. To model such a process in the midst of a free-fall collapse therefore requires a fully three-dimensional, nonlinear hydrodynamical simulation with adequate spatial resolution. Smoothed-particle hydrodynamic (e.g., Lucy 1977, Benz 1991, Monaghan 1992) and finite-difference hydrodynamic (e.g., Boss & Mayhill 1992, Truelove et al. 1998) techniques have both been successfully employed to study various aspects of this problem. With either of these techniques the system is advanced forward in time via an explicit (rather than implicit) integration of the time-dependent equations that govern the evolution of self-gravitating fluids. Hence, both techniques are constrained by the Courant-Freidrichs-Lewey condition (Courant et al. 1928; see also p. 45 of Roache 1976) to take time steps that are very small compared with the physical system's sound-crossing time, free-fall time, and rotation period. This means many integration time steps are required to model fragmentation, even for systems that fragment promptly. Then when you consider how many grid cells (in finite-difference hydrodynamic techniques) or particles (in smoothed-particle hydrodynamic techniques) are required to adequately resolve a fragmentation event (Truelove et al. 1997, 1998; Whitworth 1998), it becomes clear that each modeled event requires a very large amount of computing resources. With these available simulation tools it is usually impractical to examine mechanisms that might lead to the breakup of a cloud only after a significant evolutionary delay (see discussion in "Delayed Breakup," below).

Many different groups have utilized three-dimensional hydrodynamical techniques to study the early, approximately free-fall phase of the collapse of rotating,

Jeans-unstable gas clouds in an effort to see whether prompt fragmentation occurs. Generally an isothermal ( $\gamma = 1$ ) equation of state has been assumed because, as illustrated in Figure 2, that is what appears to be appropriate for the early phases of collapse (Boss & Bodenheimer 1979, Tohline 1980, Boss 1980, Bodenheimer et al. 1980, Różyczka et al. 1980, Gingold & Monaghan 1981, Wood 1982, Miyama et al. 1984, Monaghan & Lattanzio 1986, Bonnell et al. 1991, Burkert & Bodenheimer 1993, Sigalotti 1997, Truelove et al. 1998, Tsuribe & Inutsuka 1999). However, some attempts have been made to include the effects of adiabatic compression and heating at intermediate densities (Boss 1986, Myhill & Kaula 1992, Bonnell & Bate 1994b, Bate 1998, Tsuribe & Inutsuka 2000) or to focus just on the likelihood of prompt fragmentation in adiabatic collapse regimes (Boss 1981, Arcoragi et al. 1991). Before reviewing what has been learned about prompt fragmentation from these investigations, it is useful to summarize the general behavior of a cloud's collapse based on some of the general principles outlined above in "Basic Physical Principles." For clarity, we use the subscript  $cl$  to identify global properties of the cloud that do not change with time, such as the cloud's total mass  $M_{cl}$  and total angular momentum  $J_{cl}$  and the subscript (or sometimes superscript)  $i$  to denote the initial properties of the cloud at the onset of its collapse.

## Nearly Homologous Collapses

If a rotating cloud begins to collapse from a spherical or spheroidal configuration that is uniform in density and whose mass  $M_{cl}$  is significantly larger than the local Jeans mass  $M_J^i$ —that is, from a configuration in which  $\alpha_i \ll 1/2$ —then the cloud collapses fairly homologously. On a free-fall timescale  $\tau_{ff}^i$  governed by its initial mean density  $\bar{\rho}_i$ , the cloud evolves through a sequence of flatter and flatter configurations, not unlike the collapsing pressure-free spheroids modeled some time ago by Lynden-Bell (1962, 1964), Lin et al. (1965), and Hutchins (1976). Indeed, because the ratio of thermal to gravitational energy  $\alpha$  drops during the isothermal phase of collapse (see Equation 30), the local Jeans mass also steadily decreases and the cloud more and more closely approximates a pressure-free spheroid.

As the cloud's evolutionary time  $t$  approaches one initial free-fall time  $\tau_{ff}^i$  and its degree of flattening becomes most extreme, pressure gradients build to the point at which they are able to decelerate the collapse—at least in the vertical direction. If the cloud's angular momentum  $J_{cl}$  is sufficiently large, this deceleration of the collapse will occur while the cloud is still in the isothermal phase of its contraction. As a result (see the discussion in "The Importance of the Effective Adiabatic Exponent  $\gamma$ ," above), the cloud will necessarily be very flat and  $\beta$  will have grown to a value close to  $1/2$ . If the cloud's total angular momentum is relatively small, the cloud can enter an adiabatic phase of its contraction before the collapse begins to decelerate. In this case as well, however, the homologously collapsing cloud is destined to be very flat when the deceleration occurs because  $\alpha$  will have dropped to a very small value during the cloud's earlier, isothermal phase of contraction.

Using Equation 29, one can estimate the radial size (and the mean density) of such a flattened configuration (Tohline 1981, Hachisu & Eriguchi 1985).

Note that in a homologously contracting cloud, virtually all of the cloud's mass reaches the final, flattened configuration at approximately the same time. That is, at approximately one free-fall time, the accretion rate  $\dot{M}$  becomes very high, but there is not an extended phase of accretion thereafter. The early, spherically symmetric simulation by Narita et al. (1970) presents a nonrotating analog to this type of evolution; the collapse started from a configuration in which  $\alpha_i$  was relatively small, and after a central equilibrium core formed, the core experienced only a brief period of relatively rapid accretion (and a correspondingly high accretion luminosity).

## Nonhomologous Collapses

If, on the other hand, a cloud begins to collapse from a configuration that is fairly centrally condensed and/or the cloud initially is only marginally Jeans unstable (that is,  $\alpha_i \lesssim 1/2$ ), then the collapse proceeds in a nonhomologous fashion. The central region of the cloud collapses ahead of the rest of the cloud, producing a steep central density gradient. If the cloud is initially centrally condensed, this happens because, at every position in the cloud the timescale for collapse is governed by the "local" free-fall time; regions of higher mean density have shorter free-fall times, so the central region runs away from the rest (e.g., Section 3.2 of Tohline 1982). If the cloud is only marginally Jeans unstable initially, this happens because  $\tau_s^i \approx \tau_{\text{ff}}^i$  (see the discussion associated with Equation 23). A rarefaction wave propagating in from the edge of the cloud reaches the cloud center in approximately one free-fall time and establishes a relatively steep density gradient in its wake (Bodenheimer & Sweigart 1968, Larson 1969, Penston 1969).

As a result, a relatively small volume of material at the core of the cloud will have an opportunity to find an equilibrium configuration first (locally, at least,  $\alpha + \beta \approx 1/2$ ), then that configuration will change with time as material (and angular momentum) from the rest of the cloud accretes onto the core. However, as explained above in "The Importance of the Effective Adiabatic Exponent  $\gamma$ ," as long as the core remains isothermal it will be unable to settle into an equilibrium state without the aid of rotation. If there is enough angular momentum in the cloud's core, the core's collapse can be stopped by rotation in the isothermal phase; in this case the first equilibrium core will necessarily exhibit a large value of  $\beta$ . Otherwise, the cloud's core must contract to a density regime (see Figure 2) in which  $\gamma > 4/3$  before it finds its initial equilibrium configuration. In either case, owing to the nonhomologous nature of the collapse, the first equilibrium core will contain a relatively small fraction of the entire cloud's mass, and an extended period of mass accretion will follow the core's formation. The early spherically symmetric simulation by Larson (1969) presents a nonrotating analog to this type of evolution.

It is important to note that the key timescales associated with the first equilibrium core ( $\tau_{\text{ff}}^{ec}$ ,  $\tau_s^{ec}$ , and  $\tau_{\text{rot}}^{ec}$ ) all generally will be very short compared with the initial



free-fall time  $\tau_{\text{ff}}^i$  of the cloud and, hence, short compared with the core's accretion timescale  $\tau_{\text{accrete}}^{ec}$ . This is because, as shown in “Key Timescales” and “Implications of the Virial Theorem,” above, all three of these key timescales are shorter in higher density configurations, and the density of the collapsed core  $\bar{\rho}_{ec}$  is necessarily higher (usually much higher) than the cloud's original mean density  $\bar{\rho}_i$ . (See Table 1 and the uppermost axis of Figure 2 for values of the dynamical timescale—specifically, the orbital period—that correspond to various density regimes.) For example, the first core that formed in Larson's (1969) simulations had a mean density that was approximately 5 orders of magnitude higher than the cloud's initial density, so the core's sound-crossing time and local free-fall time were roughly 2.5 orders of magnitude shorter than the cloud's initial free-fall time. Therefore, in a dynamical sense, the core will be relatively isolated from its surroundings. If the core is found to be unstable toward the development of a dynamical instability (characterized by an e-folding time that is of order the local free-fall time  $\tau_{\text{ff}}^{ec}$ ), this instability has an opportunity to manifest itself and even grow to nonlinear amplitude before the core is significantly influenced by further accretion from the surrounding cloud material.

## Does Prompt Fragmentation Occur?

All of the three-dimensional hydrodynamical simulations that have been conducted to date to investigate prompt fragmentation in collapsing protostellar gas clouds support the following conclusion: Fragmentation does not occur during a phase of free-fall collapse. If fragmentation occurs at all, it happens only after one initial free-fall time, that is, after the cloud—or at least the core of the cloud—has collapsed into a rotationally flattened, quasi-equilibrium configuration (see discussion below). This finding argues strongly against the idea of “hierarchical” fragmentation that was proposed by Hoyle (1953) to explain how clusters of stars might form in less than a free-fall time. At first this result was somewhat surprising because linear stability analyses of the pressure-free collapse of spherical (Hunter 1962, Mestel 1965) and spheroidal (Silk 1982) gas clouds lent some support to Hoyle's idea. However, as numerical simulations have become more and more refined (e.g., Truelove et al. 1998; Bate 1998; Tsuribe & Inutsuka 1999, 2000), this result has been repeatedly reaffirmed. The presence of finite gas pressure and, more to the point, nonzero gas pressure gradients in a collapsing protostellar gas cloud is apparently what makes all the difference. (See Section 7 of Tohline 1982 for a more exhaustive discussion of this issue.)

On the other hand, multidimensional collapse simulations have shown that fragmentation of a rotating gas cloud can occur immediately after the cloud (or at least the cloud's core) has settled into its first rotationally flattened, quasi-equilibrium configuration. As Tsuribe & Inutsuka (1999, 2000) have summarized, fragmentation seems to occur relatively easily in clouds that have collapsed in a nearly homologous fashion; in contrast to this, simulations of nonhomologous collapses generally have not resulted in prompt fragmentation. Attempts have been made to

develop a formula (in terms of the cloud's initial values of  $\alpha_i$  and  $\beta_i$ , for example) that readily predicts under what specific circumstances prompt fragmentation will or will not occur (Tohline 1981, Hachisu & Eriguchi 1984, Miyama et al. 1984, Tsuribe & Inutsuka 2000). Generally speaking, these attempts have met with only marginal success. This is, perhaps, not surprising considering that hydrodynamical flows can be extremely sensitive to initial conditions and that the available parameter space for initial cloud conditions is huge. For a given choice of  $\alpha_i$  and  $\beta_i$ , for example, one can select different initial radial density profiles, distributions of angular momentum, geometries for the cloud (e.g., spherical, oblate, prolate), amplitude and shape of nonaxisymmetric perturbations, degrees of internal turbulent motions, and influences from an external environment. In addition, it has become clear that the end results can depend sensitively on numerical resolution—to the extent that many of the simulations of strictly isothermal collapse carried out prior to 1997 may have produced misleading results (Truelove et al. 1997, 1998; Boss et al. 2000).

All in all, though, the general conclusions drawn by Tsuribe & Inutsuka (1999, 2000) are likely to remain intact. They make sense on simple physical grounds. When the initial conditions are chosen in such a way that a cloud is able to collapse in a nearly homologous fashion, fluctuations that contain more than one  $M_J$  of material can amplify to some degree during the collapse (Hunter 1962). Furthermore, the cloud as a whole will evolve to an equilibrium configuration that is highly susceptible to the further growth of these, if not other, nonaxisymmetric perturbations: The parameter  $\alpha$  is very small, so the configuration contains many Jeans masses;  $\beta$  is so high that the configuration is likely to be unstable to one or more global, nonaxisymmetric instabilities, akin to the unstable modes that are present in Maclaurin spheroids (see discussion, below), and the Toomre  $Q$  parameter (Toomre 1964) is likely to be very small, making the rotationally flattened configuration susceptible to the same types of instabilities observed in galaxies.

On the other hand, a nonhomologous collapse discourages fragmentation. Even during a phase of isothermal collapse the development of radial pressure gradients retards the growth of fluctuations (Hunter 1962). Because the first equilibrium core that forms will contain only a small fraction of the total cloud mass,  $\alpha$  will be relatively high in the core, so it will be much less susceptible to the growth of nonaxisymmetric perturbations of the types just mentioned.

## Are Binaries the Result?

Although numerical simulations have demonstrated that the free-fall collapse of a rotating protostellar gas cloud can produce a flattened configuration that is susceptible to prompt fragmentation, it is not yet clear how often this process will directly produce a binary system (as opposed to producing a larger number of fragments, for example). The outcome may be sensitive to the spectrum of fluctuations present in the initial cloud state. Even when it seemed likely from early calculations that some specific sets of initial conditions would directly produce binaries, the results

are being called into question (Tsuribe & Inutsuka 1999, Boss et al. 2000). More importantly, owing to the constraints imposed by present numerical schemes, few simulations have been able to follow an individual cloud's evolution very far beyond the initial instant of fragmentation. For example, published results that purport to show the formation of a binary virtually never follow the binary through even one full orbit. It is therefore impossible to deduce (a) whether either (or both) of the components will undergo an additional fragmentation event, (b) whether or not the components will subsequently merge, or (c) how any subsequent phase of accretion will affect the parameters of the binary (e.g., period, eccentricity, mass ratio). We clearly still have a lot to learn about the relationship between prompt fragmentation and the formation of binary stars.

## DELAYED BREAKUP

As discussed above, the dynamical collapse of a Jeans-unstable, rotating gas cloud may often end with the formation of an equilibrium configuration that is stable against fragmentation. This is especially true of collapses that occur in a non-homologous fashion. Even when prompt fragmentation occurs, the individual fragments may initially be found to be stable against further fragmentation. We should then investigate whether, through its subsequent "slow" evolution toward the main sequence, such a configuration will become susceptible to breakup and thereby produce a binary system.

This equilibrium configuration (hereafter, referred to as a "core" or referenced by the subscript "ec") will be rotating, although not necessarily rapidly; it generally will contain only a small fraction of the cloud's total mass (remember that the first core that formed in Larson's 1969 nonrotating models contained only a few Jupiter masses of gas); and it may or may not initially be surrounded by a rotationally supported (accretion) disk. For the purpose of discussion, we will assign to this core a mass  $m_{ec} \ll M_{cl}$ , an equatorial radius  $R_{ec}$ , a mean temperature  $T_{ec}$ , and a mean angular velocity  $\omega_{ec}$ . From these quantities we can, in turn, determine many other key properties of the core—such as  $\rho_{ec}$  and  $\beta_{ec}$ —via the expressions given in "Basic Physical Principles," above.

In the context of this discussion of delayed breakup, the phrase "slow evolution" is intended to convey the idea that the core is no longer in free-fall collapse and that its overall structure is not changing significantly on a free-fall time  $\tau_{ff}^{cc}$ , as measured by the core's mean density. Keep in mind, however, that this evolution may still be fast compared with the cloud's initial free-fall time  $\tau_{ff}^i$  because  $\bar{\rho}_{ec} \gg \bar{\rho}_i$ . In the absence of significant nonaxisymmetric distortions, the core's evolution should be driven primarily by the same two processes that have been found to be important in spherically symmetric models of cloud collapse: radiation losses and accretion (see, for example, the detailed description provided by Winkler & Newman 1980). Both processes cause the mean density and the mean temperature of the core to steadily rise, along an evolutionary trajectory like the one displayed in Figure 2.

In the case of a rotating core it is clear by Equation 29 that as the core's density increases,  $\beta_{ec}$  increases as well.

The core's mass  $m_{ec}$  will steadily increase through accretion of material that is either falling directly in from the cloud or migrating in from a surrounding disk. The core's total angular momentum will steadily increase as a result of accretion as well. Normally, the accretion process will add relatively high specific angular momentum material to the core because there is a natural tendency for the cloud's low specific angular momentum material to accumulate in the core first. Accretion will therefore tend to increase the ratio of the core's rotational to gravitational energy,  $\beta_{ec}$ , faster than one would have expected from the core's contraction alone. And if the core is not initially surrounded by a disk, one will almost certainly develop as a result of direct infall from the cloud (see Cassen & Moosman 1981, Terebey et al. 1984, and Section 4.1.3 of Shu et al. 1987).

In the following subsections, we examine the stability of an equilibrium core as it undergoes slow evolution of the type described above. Then we examine the stability of the accretion disk that surrounds such a core. More specifically, we examine whether nonaxisymmetric instabilities might arise in either the core or its accompanying disk that would lead to the "delayed breakup" of the protostellar cloud into a binary star system.

## Nonaxisymmetric Instabilities in Rapidly Rotating, Equilibrium Cores

As a result of accretion and radiation losses, a rotating equilibrium core will contract and become more rapidly rotating, in the sense that  $\beta_{ec}$  will steadily increase. When discussing the stability of such a system, it is useful to refer to a diagram, such as the one presented here in Figure 3 (see also Figure 15 of Chandrasekhar 1969 and Figure 1 of Durisen & Tohline 1985), in which one can identify rotating ellipsoidal configurations of any shape. In particular, for an ellipsoid with principal axes  $(a_1, a_2, a_3)$  and rotation about its  $a_3$ -axis, the ordinate of Figure 3 ( $a_3/a_1$ ) specifies the object's degree of rotational flattening, and the abscissa ( $a_2/a_1$ ) specifies the degree of the configuration's equatorial ellipticity. For example, the point in the upper right-hand corner (marked by an  $S$ ) identifies a sphere; points along the right-hand, vertical axis (passing from  $S$  through the points marked  $M_2$  and  $O_2$ ) identify flattened, axisymmetric (oblate spheroidal) configurations; the curves connecting points  $S$ ,  $M_2$ , and  $O_2$  to the origin identify sequences of more and more distorted ellipsoids.

Strictly speaking, Figure 3 can be used to accurately identify the properties of ellipsoidal figures of equilibrium that arise only for uniform-density objects with velocities that are linear functions of the coordinates. In this context, the right-hand vertical axis represents the sequence of uniformly rotating, Maclaurin spheroids, and the three curves connecting the Maclaurin sequence to the origin specify certain subsets of the general class of Riemann ellipsoids. We have adopted the conventions used by Chandrasekhar (1969) and Lebovitz (1974) in labeling key bifurcation

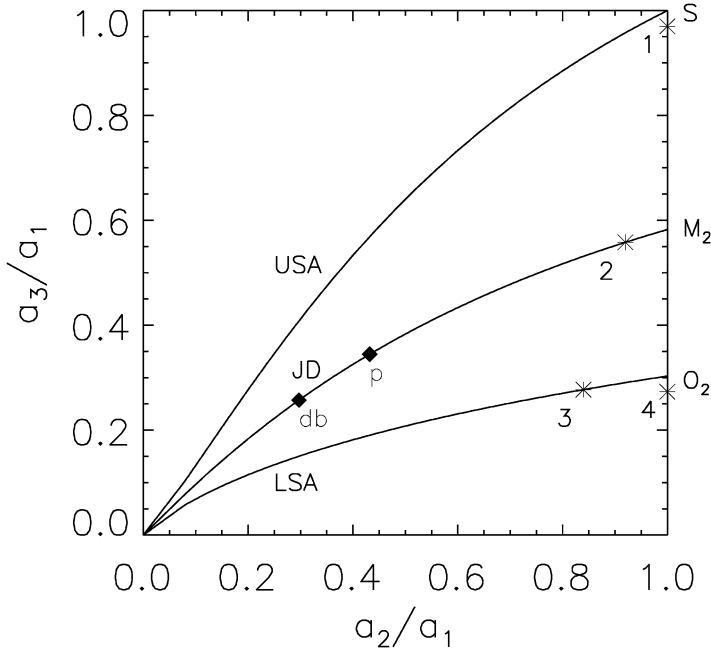


**Figure 3** A phase-space diagram for ellipsoidal configurations with principal axis lengths ( $a_1, a_2, a_3$ ). Figures are rotating about the  $a_3$ -axis. The right-hand vertical axis represents the sequence of rotationally flattened Maclaurin spheroids ( $a_2 = a_1$ ). The three curves connecting this vertical axis to the origin represent three separate sequences of Riemann S-type ellipsoids: USA, the upper self-adjoint ( $x = -1$ ) sequence; JD, the Jacobi-Dedekind sequence; LSA, the lower self-adjoint ( $x = +1$ ) sequence. Key bifurcation points along the Maclaurin sequence are labeled by  $M_2$  and  $O_2$ . Along the Jacobi ellipsoid sequence, bifurcation points to the pear-shaped (p) and dumbbell (db) sequences are also marked. The data used to construct this plot has been drawn directly from Chandrasekhar (1969).

points along the Maclaurin sequence and in labeling the key ellipsoidal sequences: USA is the upper ( $x = -1$ ) self-adjoint series of Riemann S-type ellipsoids; it branches off of the Maclaurin sequence at  $\beta = 0$ . JD refers to the Jacobi-Dedekind sequence; it bifurcates from the Maclaurin sequence at  $\beta = 0.1375$ . LSA is the lower ( $x = +1$ ) self-adjoint series of Riemann S-type ellipsoids; it bifurcates from the Maclaurin sequence at  $\beta = 0.2738$ . In a less formal way, however, it also is useful to refer to Figure 3 when discussing the evolution of less idealized (e.g., centrally condensed and differentially rotating) configurations that more closely resemble real protostellar cloud cores.

In the context of Figure 3, a slowly contracting cloud core will move down along the right-hand vertical axis from, e.g., point 1 toward the bifurcation point marked

$M_2$ . However, the cloud core will be unable to become arbitrarily flat and maintain an axisymmetric structure. Stability analyses (e.g., Lyttleton 1953, Chandrasekhar 1969, Tassoul 1978, Durisen & Tohline 1985) tell us that after reaching a critical degree of flattening (that is, a critical value of  $\beta_{ec}$ ) the cloud will begin to distort into a rotating bar-like (ellipsoidal) configuration that has a lower total energy.

**CLASSICAL VIEW OF FISSION** If the equilibrium core's contraction occurs on a timescale that is long compared with the viscous dissipation timescale of the gas, then the core will begin to deform into a triaxial configuration when it acquires the degree of flattening identified by the point identified as  $M_2$  in Figure 3, that is, once the rotational energy of the core climbs to a value of  $\beta_{ec} \approx 0.14$ . Thereafter, further contraction should drive the evolution along the JD sequence toward, for example, point 2 in Figure 3. As the cloud evolves beyond this point on the JD sequence and becomes even more elongated, stability analyses tell us that it will become susceptible toward even higher-order figure deformations. In particular, as Lyttleton (1953) has reviewed, from the nineteenth and early twentieth century works of Poincaré, Darwin, Liapounoff, Jeans, and Cartan, it has been known for over 100 years that ellipsoids along the JD sequence become susceptible to a pear-shaped deformation at the point marked p in Figure 3; and these ellipsoids are susceptible to a dumbbell-shaped deformation at the point marked db. More recently, Eriguchi et al. (1982) have explicitly demonstrated that a sequence of pear-shaped configurations and a sequence of dumbbell-shaped configurations bifurcate at the points p ( $a_2/a_1 = 0.432$ ;  $a_3/a_1 = 0.345$ ;  $\beta = 0.1268$ ) and db ( $a_2/a_1 = 0.297$ ;  $a_3/a_1 = 0.258$ ;  $\beta = 0.1863$ ), respectively. Very early on, the realization that a pear-shaped sequence branches off of the Jacobi sequence "gave rise to the notion that if the mass were stable and evolved by equilibrium forms along this [pear-shaped] series, with the furrow continually deepening as the figure elongated, the final result would be two detached masses rotating in circular orbital motion about each other" (Lyttleton 1953, p. 3). This is the classical formulation of the "fission" theory of binary star formation.

It is discouraging to realize that, more than 100 years after its formulation, the full, nonlinear evolutionary scenario that underpins this classical theory of fission has never been fully tested. That is, to date, nobody has evolved a uniform-density, uniformly rotating ellipsoid slowly along the JD sequence to see whether it spontaneously deforms into a pear-shaped configuration and then whether the slow contraction of the "pear" leads to its breakup. There are, however, a number of reasons why the astrophysical community has decided that this classical fission scenario will not work.

First, it has been determined by stability analyses that ellipsoids are dynamically (rather than secularly) unstable toward the pear-shaped deformation at all points beyond point p on the Jacobi (JD) sequence (Lyttleton 1953). Hence, any attempt to slowly evolve a configuration beyond this critical point of bifurcation will almost certainly cause the configuration to depart rapidly from the desired sequence of uniformly rotating pears. Second, the sequence of pear-shaped configurations discovered by Eriguchi et al. (1982) shows no sign of developing a

“deepening furrow,” but rather, terminates by equatorial mass-shedding. Third, it is now generally accepted that the viscosity of protostars is too low for viscous dissipation to drive evolution along the JD sequence (Lynden-Bell 1964, Lebovitz 1974) in the first place. That is, the contraction of protostellar cloud cores almost certainly occurs on a timescale that is short compared with the viscous dissipation timescale. For these reasons the classical theory of fission has been abandoned as an explanation of how binary stars form.

**LEBOVITZ'S REVISED VERSION OF THE FISSION THEORY** With a thorough understanding of the classical theory's shortcomings, Lebovitz (1974, 1984) has proposed a revised formulation of the classical fission hypothesis. It parallels the classical theory in that the rotating cloud core slowly contracts along a sequence of axisymmetric (or at least approximately axisymmetric) spheroids; then, at a critical degree of flattening, the evolution shifts to a family of more and more elongated ellipsoids. The difference is that Lebovitz considers the evolution of inviscid configurations (acknowledging the idea that contraction times are short compared with viscous times). As a result, the relevant bifurcation point off of the axisymmetric spheroidal sequence is the point marked  $O_2$  in Figure 3, and the relevant ellipsoidal sequence is the one labelled LSA. Instead of following an evolutionary trajectory that progresses from point 1 in Figure 3 to a point on the JD sequence, the core will evolve as an axisymmetric structure through the location labeled  $M_2$ , continuing to flatten until it reaches the bifurcation point marked  $O_2$ . At this point ( $\beta_{ec} \approx 0.27$ ) the equilibrium core will deform into an ellipsoidal structure and, upon further contraction, it will evolve along the sequence labeled LSA toward, for example, point 3 in Figure 3.

As explained by Lebovitz (1974, 1984, 1989), this evolutionary scenario potentially avoids all of the objections that have been raised in the context of the classical fission hypothesis. First, it does not matter that the viscous timescale is long compared with the contraction timescale in protostellar clouds because deformation into an ellipsoidal configuration occurs in the absence of viscosity. Second, on the direct LSA sequence (see Lebovitz 1974) the order of the points p and db are reversed from their positions on the JD sequence, so by evolving along this sequence the cloud can avoid altogether problems that might be associated with third-harmonic (pear-shaped) instability. Because Eriguchi & Hachisu (1985) have shown that dumbbell-binary sequences do exist and that they bifurcate smoothly from sequences of Riemann ellipsoids, it is tempting to suggest that further slow contraction of the equilibrium core will drive it smoothly along a dumbbell sequence to a binary configuration. This is the essence of Lebovitz's revised version of the fission theory.

A number of questions remain to be answered before the viability of Lebovitz's revised theory can be properly assessed. Most importantly, it has not been demonstrated whether bifurcation from the relevant ellipsoidal sequence to a dumbbell sequence occurs stably and, if it does, whether continued slow contraction of the configuration will actually proceed smoothly to a binary configuration, as envisioned by Eriguchi & Hachisu (1985).

## Direct Breakup from an Axisymmetric State

Both the original and revised version of the fission hypothesis of binary star formation have grown out of the expectation that a slowly contracting, equilibrium cloud core will deform from an axisymmetric structure into a triaxial (bar-like) configuration that is dynamically stable. Fission is hypothesized to occur only after this triaxial configuration has undergone further slow contraction. These ideas have not been fully tested in the context of realistic protostellar clouds largely because it has not been possible to construct equilibrium models of rapidly rotating, triaxial configurations with realistic (compressible) equations of state. In the absence of such equilibrium models, we cannot even begin to examine the critical questions of stability that are at the root of these two fission hypotheses. (As discussed in “Slow Contraction of a Rapidly Rotating Ellipsoid,” below, some relief to this situation may be forthcoming.)

However, we do have the tools in hand to construct equilibrium models of rapidly rotating, axisymmetric configurations with realistic equations of state and a wide variety of different distributions of angular momentum (e.g., Hachisu 1986). Over the past 15 years a considerable amount of work has been directed toward understanding the stability properties of these axisymmetric systems (Tohline et al. 1985, Williams & Tohline 1987, Luyten 1990, Pickett et al. 1996, Toman et al. 1998, Shibata et al. 2000). Through these studies, for example, it has been determined that virtually all axisymmetric configurations are dynamically unstable toward the development of a “barmode” structure if  $\beta_{ec} \geq 0.27$ . This finding overlaps well with the classical stability analysis of Maclaurin spheroids, wherein a bifurcation to the LSA sequence of Riemann ellipsoids occurs at  $\beta = 0.2738$  (the point marked  $O_2$  in Figure 3). It is in this sense that Figure 3 provides a useful context in which to discuss the evolutionary trajectories of slowly contracting, protostellar gas clouds even though it was originally constructed from studies of much simpler (e.g., uniform density, incompressible) equilibrium structures.

In addition, hydrodynamical codes (like the ones developed to study the prompt fragmentation problem) have been used extensively to determine whether or not the nonlinear development of this barmode instability results directly in the breakup of an equilibrium cloud core (Tohline et al. 1985, Durisen et al. 1986, Williams & Tohline 1988, Pickett et al. 1996, New et al. 2000, Cazes & Tohline 2000, Brown 2000). The initial model used in these investigations generally has been a structure that sits on the axisymmetric sequence and just beyond the point (marked  $O_2$  in Figure 3), where inviscid systems are expected to evolve dynamically away from an axisymmetric structure—that is, starting from a point like point 4 in Figure 3. From all of these investigations, the unanimous consensus is that breakup does not occur (see Tohline & Durisen 2001 for a recent overview). Instead, within a few rotation periods  $\tau_{\text{rot}}$  the cloud core generally deforms into a bar-like structure with a slight two-armed spiral character; gravitational torques quickly facilitate a local redistribution of angular momentum within the core (Imamura et al. 2000); a relatively small amount of high specific angular momentum material is shed in the equatorial



plane; and the core settles down into a dynamically stable, roughly ellipsoidal bar that is spinning about its shortest axis. As Cazes & Tohline (2000) discussed in detail, when viewed from a frame rotating with this bar, it is clear that the structure is very robust and supports nontrivial internal motions. In a qualitative sense, the bar resembles a Riemann ellipsoid with a structure similar to the one identified by point 3 on the LSA sequence in Figure 3. Hence, Cazes & Tohline (2000) referred to the configuration as a “compressible analog of a Riemann Ellipsoid.”

These nonlinear investigations of the development of the bar-mode instability from initially axisymmetric configurations also have been categorized as “fission studies” (e.g., Durisen & Tohline 1985). Because there is unanimous agreement that such evolutions do not lead directly to the formation of a binary system, there has been a broad pronouncement that the fission hypothesis is dead (Boss 1988, Bodenheimer et al. 1993, Bonnell 2001). This pronouncement seems premature, however. Neither the classical fission theory nor the revised one proposed by Lebovitz predicted that fission would occur directly from an instability that arises in axisymmetric configurations. Instead, as summarized above, the expectation was that a slowly contracting, equilibrium cloud core would deform first into a triaxial (bar-like) configuration. Fission should then occur only after the triaxial configuration undergoes further slow contraction past a point at which the structure becomes unstable to a higher-order surface distortion.

## Slow Contraction of a Rapidly Rotating Ellipsoid

It has proven difficult to critically evaluate this last step of the classical or revised fission hypothesis because few models of equilibrium, triaxial configurations exist for systems with a physically relevant, compressible equation of state. A limited set of rigidly rotating, polytropic bars have been constructed for very slightly compressible fluids (Vandervoort & Welty 1981, Ipser & Managan 1981, Hachisu & Eriguchi 1982), but focusing on Lebovitz’s scenario in particular, no one has yet figured out how to routinely construct compressible models of rotating ellipsoids that are spinning fast enough to serve as analogues to the Riemann ellipsoids that lie along the LSA sequence in Figure 3.

As just summarized, however, groups that have modeled the nonlinear development of the bar-mode instability in rapidly rotating, axisymmetric gas clouds have discovered that, after shedding a bit of material in the equatorial plane, the system usually settles down into a steady-state bar. Also, as Cazes & Tohline (2000) have pointed out, this bar in many respects serves as a compressible analog of the Riemann ellipsoids (CARE). With Lebovitz’s revised fission hypothesis in mind, Cazes (1999; see also Tohline & Durisen 2001) slowly cooled one of these CAREs, following its cooling evolution in a self-consistent fashion with a finite-difference hydrodynamic code. Because the gas was being modeled as a polytrope, cooling was accomplished by slowly decreasing the system’s polytropic constant,  $K$ , according to the relation  $K = K_0(1 - t/\tau_{\text{cool}})$  with  $\tau_{\text{cool}} = 4P_{\text{pattern}}$ , where  $P_{\text{pattern}}$  was the initial pattern rotation period of the bar. The configuration slowly contracted

and began to spin somewhat faster, as expected, and it also became somewhat more elongated. Roughly speaking, from a configuration like point 3 in Figure 3, the system slowly evolved to the left along the LSA sequence. Then, after  $K$  had decreased to approximately half of its original value, the model began to oscillate dynamically between a centrally condensed, bar-like state and a distinctly dumbbell shape. In its dumbbell state the model presented a pair of clearly defined off-axis density maxima and a velocity field that showed circulation about each density maximum. Evidently the bar had reached a point in its evolution along the LSA sequence where there were two equally plausible equilibrium configurations into which it was permitted to settle. Cazes (1999) hypothesized that upon further cooling the system was likely to evolve along a dumbbell-binary sequence analogous to the one depicted by Eriguchi & Hachisu (1985) and through a common-envelope binary state like the one discussed by Tohline et al. (1999).

Unfortunately, owing to computational constraints, Cazes was unable to follow his cooling evolution further, and when cooling was stopped the model settled into a centrally condensed, rather than a binary, configuration. Thus, it is debatable whether Cazes' model was actually progressing along a route to fission, but his simulation provides tantalizing evidence that Lebovitz's revised fission hypothesis may be correct under certain circumstances.

## Stability of Accretion Disks

After an equilibrium core forms at the center of a collapsing gas cloud, it will continue to grow in mass through the direct accretion of infalling cloud material, but the core will be able to directly accrete only the cloud material that has relatively low specific angular momentum. Specifically, only material that arrives at the surface of the core with an angular velocity  $\lesssim \omega_{\max}^{ec}$ , as given by Equation 24, will be gravitationally bound to the core. For a core of radius  $R_{ec}$  this means that only material with a specific angular momentum  $j < j_{\max}^{ec} \approx R_{ec}^2 \omega_{\max}^{ec}$  will fall directly onto the core. The rest of the infalling material must form or become part of a centrifugally supported disk that surrounds the core. For purposes of illustration we have listed in Table 2 the value of  $j_{\max}^{ec}$  that is associated with the equilibrium core that will form during a spherically symmetric collapse at the points marked B, C, and D along the evolutionary path shown in Figure 2. (In each case,  $R_{ec}$  has been estimated by treating the core as a sphere of mass  $M_{\text{equil}}$  and mean density  $\rho$  as given in Table 2.)

In practice, unless the molecular gas cloud is initially very slowly rotating, only a small fraction of the cloud's gas will have  $j < j_{\max}^{ec}$ . Consider, for example, the canonical uniform-density, spherical gas cloud that is initially rotating with an angular velocity  $\omega_i$  and, hence, initially has a ratio of rotational to gravitational potential energy  $\beta_i = \frac{1}{2}(\omega_i/\omega_{\max}^{cl})^2$ . [Cameron (1978) and Cassen & Summers (1983) examined models of this type in the context of the formation of the solar nebula.] The specific angular momentum of the material in such a cloud increases as one moves out from the center of the cloud. Specifically, in terms of the fractional mass

$m_{\varpi}$  that is enclosed inside each cylindrical radius  $\varpi$ ,

$$j = \frac{5}{2} \frac{J}{M} [1 - (1 - m_{\varpi})^{2/3}] \quad (32)$$

(Hachisu et al. 1987). By inverting Equation 32, we obtain the following expression for the fraction of the cloud's material that has a specific angular momentum  $j \leq j_{\max}^{ec}$ :

$$m_{\varpi} = 1 - [1 - \eta(2\beta_i)^{-1/2}]^{3/2} \approx \eta\beta_i^{-1/2}, \quad (33)$$

where  $\eta \equiv (j_{\max}^{ec}/j_{\max}^{cl})$  and  $j_{\max}^{cl}$  is the maximum specific angular momentum that material can have in the initial, marginally Jeans-unstable gas cloud. Examining the values of  $j_{\max}^{ec}$  listed in Table 2 (and realizing that the value given for Case A supplies  $j_{\max}^{cl} = 3.6 \times 10^{21}$ ), we see that  $\eta$  ranges between  $4 \times 10^{-3}$  (Case B) and  $1 \times 10^{-4}$  (Case D). Hence, unless  $\beta_i$  is extremely small,  $m_{\varpi}$  will be very small, indicating that the majority of the cloud's mass ( $1 - m_{\varpi}$ ) will be unable to fall directly onto the central equilibrium core. One arrives at this conclusion even if the uniformly rotating cloud is initially as centrally condensed as a singular isothermal sphere (Cassen & Summers 1983, Terebey et al. 1984).

We must therefore ask, as Cameron (1978) and Cassen & Moosman (1981) did in the context of the primitive solar nebula, whether the surrounding disk of gaseous material will remain stable as an axisymmetric configuration when it accumulates as much or even more mass than the central core. Cameron was interested in the possibility that a giant gaseous proto-planet might form from a gravitational instability in such a disk. Here we are of course interested in whether an object (or more than one object) with a mass comparable to the central core might form from such a disk. With this in mind, we focus on recent studies that have examined whether or not protostellar disks are susceptible to global, nonaxisymmetric instabilities with relatively long wavelengths (low azimuthal mode numbers  $m$ ) so that their development incorporates a sizeable fraction of the gas that is in the disk.

As Shu et al. (1990) have summarized, there is a long history of research into the stability of disks in the context of galaxies, evolved stars, and planetary rings. Some of this work is relevant to discussions of the stability of protostellar accretion disks [such as the classic works of Toomre (1964) and Goldreich & Tremaine (1978)], but protostellar disks are sufficiently different from planetary rings and galaxy disks that issues related to their stability have to be addressed separately (Adams et al. 1989). Despite continuing improvements in computing resources, it is still very difficult to model with adequate spatial and time resolution the full three-dimensional evolution of protostellar disks. This is primarily because they have a significant radial extent, so the dynamical timescale governing events near the inner edge of the disk (near the surface of the protostar) can be many orders of magnitude shorter than the relevant timescale at the outer edge of the disk. The vertical thickness of the disk is also generally expected to be very small compared with the radial extent of the disk, which puts extra demands on a model's spatial resolution. As a result, the models that have been developed have either

(a) assumed that the disk is infinitesimally thin (has no vertical extent) and examined the evolution only of two-dimensional  $(\varpi, \theta)$  systems or (b) assumed that the disk has some vertical thickness but does not have a large radial extent relative to its inner edge, in which case the structure resembles a torus. The work of Papaloizou & Lin (1989) and Adams et al. (1989) have led the way in the former category of investigations; Papaloizou & Pringle (1984) and Goodman & Narayan (1988) have led the way in the latter category.

Studies of infinitesimally thin, self-gravitating disks generally have shown that, under a wide range of conditions the disk will become unstable toward the development of long-wavelength, spiral shaped instabilities if the disk-to-central-object mass ratio,  $M_d/M_c$ , is sufficiently large (Papaloizou & Lin 1989; Shu et al. 1990; Heemskerk et al. 1992; Noh et al. 1991, 1992; Laughlin & Korchagin 1996; Taga & Iye 1998). Most significantly, Adams et al. (1989) discovered that an  $m = 1$  “eccentric mode” instability arises in disks with  $M_d/M_c \gtrsim 1$  even in situations in which an evaluation of the Toomre (1964)  $Q$  parameter indicates that the growth of many other modes is suppressed. It appears as though any of the spiral modes whose relative stability is governed by the importance of self-gravity in the disk will be effective at redistributing angular momentum within the disk and, thereby, can drive accretion of disk material onto the central protostar (e.g., Laughlin & Różyczka 1996). However, the “eccentric mode” appears to be special in the sense that, through its development, a “clump” of material preferentially accumulates on one side of the disk, suggesting that a separate protostellar core may be able to form from material in the disk and remain in orbit about the original, central object. This is dynamically allowed because, as explained by Adams et al. (1989), as the  $m = 1$  distortion grows in the disk, the central protostar wanders away from the center of mass of the system along a spiral trajectory that keeps it and the clump of material in the disk on opposite sides of the system’s center of mass. With finite-difference hydrodynamical techniques, it has been difficult to follow this proposed disk fragmentation event to completion. As Laughlin & Różyczka (1996) explained following one of their simulations, before the clump became fully developed, “the central star had spiraled out and crashed into the inner disk edge, effectively terminating the computation due to numerical difficulties.” Smoothed-particle hydrodynamic simulations have been more successful at illustrating how this full fragmentation event may occur (Adams & Benz 1992, Bonnell 1994).

It is significant that all of the research on infinitesimally thin disks conducted after the insightful work of Adams et al. (1989) has confirmed that protostellar disks are susceptible to an  $m = 1$  instability if  $M_d/M_c \gtrsim 1$ ; and almost all agree that this is the first unstable mode that is likely to spontaneously develop as the mass ratio  $M_d/M_c$  grows through the accretion of infalling cloud material (see Laughlin & Różyczka 1996 for a counter-example). At present, however, there is little agreement regarding the precise physical mechanism responsible for exciting this mode—indeed, five explanations have been proposed (Shu et al. 1990, Heemskerk et al. 1992, Noh et al. 1992, Laughlin & Korchagin 1996, Taga & Iye 1998). As a result, there is little agreement regarding the precise mass ratio at which the mode first becomes unstable, although it seems in most cases to be within a

factor of a few of the value  $3/4\pi \approx 0.24$  suggested by the derivation of Shu et al. (1990).

Self-gravitating, geometrically thick disks (tori) that orbit a central point mass also appear to be unstable toward the development of long-wavelength, nonaxisymmetric modes. As Goodman & Narayan (1988) first outlined, two different types of modes appear to be excitable in addition to the “sonic” mode identified by Papaloizou & Pringle (1984) in massless accretion tori. Analogs of all three modes appear as well in “annuli,” that is, in differentially rotating systems that have limited radial extent but extend vertically to infinity (see Goodman & Narayan 1988, Christodoulou & Narayan 1992, Christodoulou 1993). Nonlinear dynamical simulations have demonstrated that radially slender tori and annuli readily distort into  $m$  clumps, where  $m$  is the mode number of the fastest growing, unstable mode (Hawley 1990, Tohline & Hachisu 1990, Christodoulou 1993, Woodward et al. 1994). For a given disk-to-central-object mass ratio  $M_d/M_c$  the relevant mode number decreases as the radial extent (thickness) of the torus increases; for a given radial extent the mode number decreases as the mass ratio decreases.

In the simulation that seems most relevant to our discussion of binary star formation, Woodward et al. (1994) evolved to nonlinear amplitude a toroidal system with  $M_d/M_c = 1$  that was unstable only toward the development of an  $m = 1$  spiral disturbance. As it grew, the distortion produced a single, high-density clump that was orbiting “about the center of mass of the system along with (but roughly oppositely positioned from) the central object,” in accordance with the behavior of the “eccentric instability” that was first discussed by Adams et al. (1989) in the context of infinitesimally thin disks. Also, as predicted, the central object moved along a spiral trajectory, progressively farther from the center of the system. Unfortunately [and reminiscent of the account given by Laughlin & Różyczka (1996)], “before the high-density blob in the disk . . . developed to the point where it clearly could be identified as a compact entity distinct from the rest of the disk material, the central object . . . impacted the inner edge of the disk.” The simulation was terminated, so it never became clear whether a binary protostellar system would be the outcome.

Andalib et al. (1997) have attempted to summarize and provide a unified discussion of these results. Generally speaking, the picture that emerges from these studies of geometrically thick disks is consistent with the one that has arisen from the studies of infinitesimally thin disks: As protostellar disks grow in mass and radius by accreting infalling cloud material, they are likely to become unstable toward the development of long-wavelength, nonaxisymmetric structure, with the so-called “eccentric mode” generally being dominant. It is therefore conceivable that some protostellar disks will break up into one or more pieces containing a sizeable fraction of the disk’s entire mass.

## SUMMARY AND CONCLUSIONS

The theory of star formation would be tremendously simplified if we could point to one physical mechanism that is primarily responsible for the transformation of single clumps of gas into binary systems. Boss (1988) has argued rather

persuasively that prompt fragmentation is the preferred mechanism and, given only meager evidence to the contrary, others have been inclined to agree (Clarke & Pringle 1993, Bodenheimer et al. 1993, Bonnell 2001). From an extensive review of the literature, I must conclude that, to date, none of the ideas that has been put forth to explain the origin of binary star systems is completely satisfactory. At the same time, I would argue that several of the ideas appear to be quite promising, but a significant amount of additional effort must be devoted toward the development of each of these ideas before any of them will become fully convincing. Before outlining the areas that require more work, let us summarize the various points on which there seems to be broad agreement.

### Issues on Which There is Broad Agreement

1. Capture holds little promise as a binary formation process. It seems clear from observations that young stars generally have paired themselves up into bound systems before they have reached stage IV in the evolutionary scenario presented by Shu et al. (1987), that is, well before they have reached the main sequence. This provides very little time for the capture process to operate because it is inherently inefficient.
2. Clouds do not fragment during a phase of free-fall collapse. This runs contrary to earliest expectations, but it seems to be borne out repeatedly by modern numerical simulations of cloud collapse that have included realistic effects of gas pressure and rotation. Instead, clouds tend to collapse to a rotationally flattened, quasi-equilibrium configuration before any fragmentation occurs, if at all.
3. Prompt fragmentation generally works immediately following a phase of free-fall collapse if a significant fraction of the cloud's mass falls into a rotationally flattened configuration approximately in unison, especially if this configuration forms while the cloud is still in the isothermal phase of its contraction (that is, while it maintains a mean density  $\lesssim 10^{-13} \text{ g cm}^{-3}$ ). Clouds are therefore susceptible to prompt fragmentation if they begin to collapse from a configuration that is relatively uniform in density and contains more than a few Jeans masses of material (i.e.,  $\alpha_i$  is well below 1/2).
4. Prompt fragmentation usually does not work if a cloud collapses in a nonhomologous fashion. Instead, a central core of relatively small mass forms first, followed by an extended phase of accretion. This core will necessarily become rapidly rotating as it accretes infalling material from the surrounding, free-falling cloud.
5. Rapidly rotating, axisymmetric cloud cores do not break up when they encounter the dynamical bar-mode instability, like the one that spontaneously arises at the bifurcation point labeled  $O_2$  in Figure 3 ( $\beta \gtrsim 0.27$ ). Instead, gravitational torques are effective at redistributing angular momentum within the core, a bit of high specific angular momentum material gets shed in the

equatorial plane, and the core settles down into a new, dynamically stable—although still rapidly rotating—configuration.

6. The core generally settles into a spinning ellipsoidal or bar-like structure after it encounters the dynamical bar-mode instability. By many accounts, the configuration appears to be a compressible analog of the Riemann ellipsoids that lie, for example, along the model sequence labeled LSA in Figure 3.
7. A substantial disk will almost certainly form around the central core through the additional infall of high specific angular momentum cloud material, and it will likely grow to a mass that is comparable to or larger than the mass of the core.
8. Protostellar disks become dynamically and globally unstable toward the development of long-wavelength, nonaxisymmetric structure when the mass contained in the disk becomes comparable to or greater than the mass of the core that it surrounds.

Out of this list, items 3, 6, and 8 provide the most promising leads in connection with our search to find the process or processes by which binary stars form. Further study is required, however, before we will be able to specify with confidence the degree to which any or all three of them is, in practice, relevant.

## Issues that Require Further Investigation

By all accounts, prompt fragmentation along the lines described in item 3, above, is a strong candidate for explaining how binaries form. Numerous simulations by many groups have demonstrated that, under the conditions described, a collapsed cloud configuration will undergo rapid, nonaxisymmetric deformation. I remain concerned about several aspects of this proposed process, however; some of these concerns are alluded to in “Does Prompt Fragmentation Occur?” and “Are Binaries the Result?”. First, to be effective, the process requires that at the onset of collapse the cloud must contain more than a few Jeans masses of material. How is nature able to construct such an artificially unstable initial configuration? Second, the outcome of the fragmentation process seems to be relatively sensitive to initial conditions. While it is true that many published simulations show the development of two fragments (or at least a strong  $m = 2$  azimuthal mode deformation), it is usually also true that some type of two-fold deformation was imposed as a form of perturbation in the initial, unstable cloud. Why should nature preferentially introduce two-fold deformations into significantly Jeans-unstable initial states? Third, few simulations have been able to follow an individual cloud’s evolution very far beyond the initial instant of fragmentation to determine whether a binary protostellar state is actually the outcome. Usually simulations are terminated before even one full orbit (and one rotation period of the initial cloud) has been completed. Fourth, collapsed cloud configurations are much less susceptible to prompt fragmentation after the gas has entered a phase of its evolution in which it heats up upon further compression, that is, at densities  $\bar{\rho} > 10^{-13} \text{ g cm}^{-3}$  (see Figure 2).

Hence, it is difficult to understand how prompt fragmentation can explain the formation of binary systems with periods shorter than about 1000 years (see the top-most horizontal axis of Figure 2).

The model developed recently by Shu et al. (2000) and Galli et al. (2001) may very well provide an answer to the first two of these concerns. It relies on the introduction of magnetic fields to support the initial cloud state and ambipolar diffusion to slowly decouple the cloud from the field so that the cloud is brought gradually to the “brink of instability.” While studying the properties of rotating gas clouds that are supported against collapse by a magnetic field, this group has found that multiple-lobed ( $m = 2, 3, 4, \dots$ ) configurations naturally bifurcate from an underlying axisymmetric sequence. Thus, it is reasonable to expect rotating clouds to already exhibit appreciable nonaxisymmetric distortions before the field decouples from the gas. Furthermore, if the field rather quickly decouples from the gas, the cloud will begin its free-fall collapse from a configuration that has a relatively small  $\alpha_i$ . Shadmehri & Ghanbari (2001) and Nakamura & Li (2001) have presented related investigations of the structure and evolution of nonaxisymmetric distortions in magnetically supported clouds.

In connection with the third concern that has been raised in the context of models of prompt fragmentation, it is clear why most numerical simulations have been terminated prematurely. Integration time steps are forced to be very small because they are linked to the free-fall (and sound-crossing) timescale associated with the densest region of a fragment, whereas the relevant orbital period is tied to the mean density of the configuration and, particularly when dealing with isothermal flows, these two timescales can become separated by many orders of magnitude. This unfortunate situation will be overcome only when we develop numerical tools that permit us to model hydrodynamical flows in three dimensions for times that are very long compared with the Courant-Freidrichs-Lewey constraint (“Prompt Fragmentation”). Until we overcome this practical limitation of our modeling techniques, we will be unable to determine (*a*) whether prompt fragmentation preferentially forms binary systems, (*b*) whether any initial fragments survive subsequent phases of accretion or merge back together, (*c*) what the final mass ratio of the binary system will be, and (*d*) whether the circum-stellar and/or circum-binary disks that form from the infalling gas indeed become massive relative to the mass of the newly formed binary cores. By building certain simplifying assumptions into their smoothed-particle hydrodynamic scheme, Bate et al. (1996) and Bate & Bonnell (1997) have begun to address this challenging but important numerical techniques problem.

In connection with item 6, above, it appears as though the results of our modeling to date are consistent with the revised fission hypothesis put forward by Lebovitz (1974, 1984) (see “Lebovitz’s Revised Version of the Fission Theory,” above). That is, rapidly rotating axisymmetric configurations that become susceptible to the dynamical bar-mode instability evolve to a configuration that, for all practical purposes, resembles a Riemann ellipsoid. In order to complete the test of this revised fission hypothesis, a method will have to be found to slowly evolve such



configurations along a sequence of more and more distorted ellipsoids (like the LSA sequence illustrated in Figure 3) to see whether the sequence eventually bifurcates to a dumbbell-binary sequence and whether slow evolution along this new sequence indeed leads to fission. As described in “Slow Contraction of a Rapidly Rotating Ellipsoid,” above, Cazes (1999) made an early attempt to model such an evolution, but his work needs to be extended; his results need to be confirmed by other research groups, and similar evolutions starting from different initial ellipsoidal states need to be investigated. The challenge will be to develop a technique by which a variety of rapidly rotating, ellipsoidal configurations can readily be constructed out of differentially rotating, compressible fluids. Numerical models of fully three-dimensional structures can be constructed one at a time by following through to completion the dynamical bar-mode instability, but this is an extremely inefficient way to proceed. More efficient methods recently have been devised to construct two-dimensional analogs of these rapidly rotating ellipsoidal configurations under certain restrictions (Syer & Tremaine 1996, Andalib 1998). Extending such techniques to three-dimensional systems would be extremely desirable.

Finally, we address the shortcomings associated with item 8, above. With few exceptions, simulations that have attempted to follow the nonlinear development of nonaxisymmetric instabilities in massive protostellar disks have run into difficulties following the evolutions to completion. This has especially been true in the case of the  $m = 1$  “eccentric instability,” which appears to be most promising in the context of the problem of binary star formation (see “Stability of Accretion Disks,” above for details). Again, dynamical range appears to be the problem. For simplicity, the protostellar core that is initially positioned at the center of the disk usually has been treated as a point mass. When the core migrates away from the center of mass of the system and impacts the disk, the simulation grinds to a halt as it tries to follow flow of the disk material into the point-mass singularity. A method needs to be devised to overcome this problem so we can determine with confidence what the outcome of this instability is; in particular, whether the disk material clumps up into a binary companion to the core. In this context, Pickett et al. (1998, 2000) have been studying the stability of systems in which the central protostar is fully resolved along with the disk. Their models have included disks with relatively modest radial extent (and therefore a relatively modest range of dynamical timescales), so they have only been able to test the viability of the eccentric mode instability in a limited way.

When examining gravitational instabilities in a protostellar disk, we must also keep in mind that viscous processes—or indeed the gravitational instability itself—acting within the disk may prevent it from ever holding a significant amount of material. Viscosity (or gravitational torques) can facilitate the radial redistribution of angular momentum within the disk and thereby allow material to move radially inward and fall onto the central protostar. If the rate of accretion of material through the disk onto the central core ever exceeds the rate of accretion of material from the surrounding gas cloud onto the disk, then the disk will decrease in mass, significantly reducing the likelihood that a binary star will form through the process

of disk fragmentation. Our understanding of the processes that lead to the formation of binary stars is therefore tightly coupled to our understanding of viscous transport processes in protostellar disks.

In conclusion, we reflect back on Mathieu's (1994) statement—supported through observations and not through theoretical models—that binary formation is the primary branch of the star formation process. Obviously nature knows how to form binary star systems. Hopefully, in the coming decade, our numerical models will find one or more fully convincing ways to do so as well.

**The Annual Review of Astronomy and Astrophysics is online at  
<http://astro.annualreviews.org>**

### LITERATURE CITED

- Adams FC, Benz W. 1992. In *Gravitational Instabilities in Circumstellar Disks & the Formation of Binary Companions*, pp. 185–94. San Francisco: Astron. Soc. Pac.
- Adams FC, Ruden SP, Shu FH. 1989. *Astrophys. J.* 347:959–76
- Alcock C, Allsman RA, Alves DR, Axelrod TS, Becker AC, et al. 2001. *Astrophys. J.* 552:259–67
- Andalib SW. 1998. *The structure and stability of selected 2-D self-gravitating systems*. PhD thesis, Baton Rouge: Louisiana State Univ.
- Andalib SW, Tohline JE, Christodoulou DM. 1997. *Astrophys. J. Suppl.* 108:471–87
- Arcoragi J-P, Bonnell I, Martel H, Benz W, Bastien P. 1991. *Astrophys. J.* 380:476–83
- Bate MR. 1998. *Astrophys. J. Lett.* 508:L95–98
- Bate MR, Bonnell IA. 1997. *MNRAS* 285:33–48
- Bate MR, Bonnell IA, Price NM. 1995. *MNRAS* 277:362–76
- Benz W. 1991. In *Late Stages of Stellar Evolution Computational Methods in Astrophysical Hydrodynamics*, pp. 259–312. New York: Springer-Verlag
- Bodenheimer P, Ruzmajkina T, Mathieu RD. 1993. In *Protostars and Planets III*, pp. 367–404. Tucson: Univ. Arizona Press
- Bodenheimer P, Sweigart A. 1968. *Astrophys. J.* 152:515–22
- Bodenheimer P, Tohline JE, Black DC. 1980. *Astrophys. J.* 242:209–18
- Bonnell IA. 1994. *MNRAS* 269:837–48
- Bonnell IA. 2001. See Zinnecker & Mathieu 2001, pp. 23–32
- Bonnell IA, Bate MR. 1994. *MNRAS* 271:999–1004
- Bonnell IA, Martel H, Bastien P, Arcoragi J-P, Benz W. 1991. *Astrophys. J.* 377:553–58
- Boss AP. 1980. *Astrophys. J.* 237:866–76
- Boss AP. 1981. *Astrophys. J.* 250:636–44
- Boss AP. 1984. *Astrophys. J.* 277:768–82
- Boss AP. 1986. *Astrophys. J. Suppl.* 62:519–52
- Boss AP 1988. *Comments Astrophys.* 12:169–90
- Boss AP, Bodenheimer P. 1979. *Astrophys. J.* 234:289–95
- Boss AP, Fisher RT, Klein RI, McKee CF. 2000. *Astrophys. J.* 528:325–35
- Boss AP, Mayhill EA. 1992. *Astrophys. J. Suppl.* 83:311–27
- Brown JD. 2000. *Phys Rev. D* 62:084024
- Burkert A, Bodenheimer P. 1993. *MNRAS* 264:798–806
- Cameron AGW. 1978. *Moon Planets* 18:5–40
- Cassen P, Moosman A. 1981. *Icarus* 48:353–76
- Cassen P, Summers A. 1983. *Icarus* 53:26–40
- Cazes JE. 1999. *The formation of short period binary star systems from stable, self-gravitating, gaseous bars*. PhD thesis, Baton Rouge: Louisiana State Univ.
- Cazes JE, Tohline JE. 2000. *Astrophys. J.* 532:1051–68

- Chandrasekhar S. 1969. *Equilibrium Figures of Equilibrium*. New Haven, CT: Yale Univ. Press
- Christodoulou DM. 1993. *Astrophys. J.* 412: 696–719
- Christodoulou DM, Narayan R. 1992. *Astrophys. J.* 388:451–66
- Clarke C. 1992. In *Complementary Approaches to Double and Multiple Star Research*, pp. 176–84. San Francisco: Astron. Soc. Pac.
- Clarke CJ, Pringle JE. 1993. *MNRAS* 261:190–202
- Close LM. 2001. See Zinnecker & Mathieu 2001, pp. 555–58
- Courant R, Friedrichs KO, Lewy H. 1928. *Math. Ann.* 100:32–38
- Di Stefano R. 2001. See Zinnecker & Mathieu 2001, pp. 529–38
- Duquenois A, Mayor M. 1991. *Astron. Astrophys.* 248:485–524
- Durisen RH, Gingold RA, Tohline JE, Boss AP. 1986. *Astrophys. J.* 305:281–308
- Durisen RH, Tohline JE. 1985. In *Protostars and Planets II*, pp. 534–75. Tucson: Univ. Arizona Press
- Eriguchi Y, Hachisu I. 1985. *Astron. Astrophys.* 142:256–62
- Eriguchi Y, Hachisu I, Sugimoto D. 1982. *Prog. Theor. Phys.* 67:1068–75
- Galli D, Shu FH, Laughlin G, Lizano S. 2001. *Astrophys. J.* 551:367–86
- Gingold RA, Monaghan JJ. 1981. *MNRAS* 197:461–75
- Goldreich P, Tremaine S. 1978. *Astrophys. J.* 222:850–58
- Goodman J, Narayan R. 1988. *MNRAS* 231:97–114
- Guilloteau S. 2001. See Zinnecker & Mathieu 2001, pp. 547–54
- Hachisu I. 1986. *Astrophys. J. Suppl.* 61:479–507
- Hachisu I, Eriguchi Y. 1982. *Prog. Theor. Phys.* 68:206–21
- Hachisu I, Eriguchi Y. 1984. *Astron. Astrophys.* 140:259–64
- Hachisu I, Eriguchi Y. 1985. *Astron. Astrophys.* 143:355–64
- Hachisu I, Tohline JE, Eriguchi Y. 1987. *Astrophys. J.* 323:592–613
- Hansen CJ, Kawaler SD. 1994. *Stellar Interiors: Physical Principles, Structure, and Evolution*. New York: Springer
- Hayashi C, Narita S, Miyama SM. 1982. *Prog. Theor. Phys.* 68:1949–66
- Hawley JF. 1990. *Astrophys. J.* 356:580–90
- Heemskerk MHM, Papaloizou JC, Savonije GJ. 1992. *Astron. Astrophys.* 260:161–74
- Hoyle F. 1953. *Astrophys. J.* 118:513–28
- Hunter C. 1962. *Astrophys. J.* 136:594–608
- Hutchins JB. 1976. *Astrophys. J.* 205:103–121
- Imamura JN, Durisen RH, Pickett BK. 2000. *Astrophys. J.* 528:946–64
- Ipser JR, Managan RA. 1981. *Astrophys. J.* 250:362–72
- Jeans J. 1919. *Problems of Cosmogony and Stellar Dynamics*. Cambridge: Cambridge Univ. Press
- Kippenhahn R, Weigert A. 1990. *Stellar Structure and Evolution*. New York: Springer-Verlag
- Larson RB. 1969. *MNRAS* 145:271–95
- Larson RB. 1990. In *Physical Processes in Fragmentation and Star Formation*, pp. 389–99. Dordrecht, The Netherlands: Kluwer
- Laughlin G, Korchagin V. 1996. *Astrophys. J.* 460:855–68
- Laughlin G, Różyczka M. 1996. *Astrophys. J.* 456:279–91
- Launhardt R. 2001. See Zinnecker & Mathieu 2001, pp. 117–21
- Launhardt R, Sargent AI, Henning Th, Zylka R, Zinnecker H. 2000. In *Birth and Evolution of Binary Stars, IAU Symp. No. 200*, ed. B. Reipurth, H. Zinnecker, pp. 103–5. San Francisco: Astron. Soc. Pac.
- Lebovitz NR. 1974. *Astrophys. J.* 190:121–30
- Lebovitz NR. 1984. *Astrophys. J.* 284:364–80
- Lebovitz NR. 1989. *Highlights Astron.* 8:129–31
- Ledoux P. 1945. *Astrophys. J.* 102:143–53
- Lin CC, Mestel L, Shu FH. 1965. *Astrophys. J.* 142:1431–46
- Lucy LB. 1977. *Astron. J.* 82:1013–24
- Luyten PJ. 1990. *MNRAS* 245:614–22

- Lynden-Bell D. 1962. *Proc. Cambridge Philos. Soc.* 58:709–11
- Lynden-Bell D. 1964. *Astrophys. J.* 139:1195–216
- Lyttleton RA. 1953. *The Stability of Rotating Liquid Masses*. Cambridge: Cambridge Univ. Press
- Marcy GW, Butler RP. 1998. *Annu. Rev. Astron. Astrophys.* 36:57–98
- Marcy GW, Butler RP. 2000. *Publ. Astron. Soc. Pac.* 112:137–40
- Mathieu R. 1994. *Annu. Rev. Astron. Astrophys.* 32:465–530
- Mayor M, Queloz D. 1995. *Nature* 378:355–59
- Mestel L. 1965. *Q. J. Roy. Astron. Soc.* 6:161–98
- Miyama SM, Hayashi C, Narita S. 1984. *Astrophys. J.* 279:621–32
- Monaghan JJ. 1992. *Annu. Rev. Astron. Astrophys.* 30:543–74
- Monaghan JJ, Lattanzio JC. 1986. *Astron. Astrophys.* 158:207–11
- Myhill EA, Kaula WM. 1992. *Astrophys. J.* 386:578–86
- Nakamura F, Li Z-Y. 2001. *Astrophys. J. Lett.* 566:L101–4
- Narita S, Nakano J, Hayashi C. 1970. *Prog. Theor. Phys.* 43:942–64
- New KCB, Centrella JM, Tohline JE. 2000. *Phys. Rev.* 62:064019
- Noh H, Vishniac ET, Cochran WD. 1991. *Astrophys. J.* 383:372–79
- Noh H, Vishniac ET, Cochran WD. 1992. *Astrophys. J.* 397:347–52
- Padgett DL, Brandner W, Stapelfeldt R, Strom SE, Terebey S, Koerner D. 1999. *Astron. J.* 117:1490–1504
- Padgett DL, Strom SE, Ghez A. 1997. *Astrophys. J.* 477:705–10
- Papaloizou JCB, Lin DNC. 1989. *Astrophys. J.* 344:645–68
- Papaloizou JCB, Pringle JE. 1984. *MNRAS* 208:721–50
- Penston MV. 1969. *MNRAS* 144:425–48
- Pickett BK, Cassen P, Durisen RH, Link R. 1998. *Astrophys. J.* 504:468–91
- Pickett BK, Durisen RH, Cassen P, Mejia AC. 2000. *Astrophys. J. Lett.* 540:L95–98
- Picket BK, Durisen RH, Davis GA. 1996. *Astrophys. J.* 458:714–38
- Portegies Z, Simon F, Hut P, McMillan SLW, Verbunt F. 1997. *Astron. Astrophys.* 328:143–57
- Quirrenbach A. 2001a. See Zinnecker & Mathieu 2001, pp. 539–46
- Quirrenbach A. 2001b. *Annu. Rev. Astron. Astrophys.* 39:353–401
- Quist CF, Lindegren L. 2000. *Astron. Astrophys.* 361:770–80
- Quist CF, Lindegren L. 2001. See Zinnecker & Mathieu 2001, pp. 64–68
- Reid IN, Gizis JE, Kirkpatrick JD, Koerner DW. 2001. *Astron. J.* 121:489–502
- Roache PJ. 1976. *Computational Fluid Dynamics*. Albuquerque, NM: Hermosa
- Różyczka M, Tscharnuter WM, Winkler K-H, Yorke HW. 1980. *Astron. Astrophys.* 83:118–28
- Shadmehri M, Ghanbari J. 2001. *Astrophys. J.* 557:1028–34
- Shibata M, Baumgarte TW, Shapiro SL. 2000. *Astrophys. J.* 542:453–63
- Shu FH. 1977. *Astrophys. J.* 214:488–97
- Shu FH, Adams FC, Lizano S. 1987. *Annu. Rev. Astron. Astrophys.* 25:23–81
- Shu FH, Laughlin G, Lizano S, Galli D. 2000. *Astrophys. J.* 535:190–210
- Shu FH, Tremaine S, Adams F, Ruden SP. 1990. *Astrophys. J.* 358:495–514
- Sigalotti LDiG. 1997. *Astron. Astrophys.* 328:586–94
- Silk J. 1982. *Astrophys. J.* 256:514–22
- Simon M, Close LM, Beck TL. 1999. *Astron. J.* 117:1375–86
- Smith KW, Bonnell IA, Emerson JP, Jenness T. 2000. *MNRAS* 319:991–1000
- Söderhjelm S. 1999. *Astron. Astrophys.* 341:121–40
- Syer D, Tremaine S. 1996. *MNRAS* 281:925–36
- Taga M, Iye M. 1998. *MNRAS* 299:1132–38
- Tassoul JL. 1978. *Theory of Rotating Stars*. Princeton, NJ: Princeton Univ. Press
- Terebey S, Shu FH, Cassen P. 1984. *Astrophys. J.* 286:529–51
- Tohline JE. 1980. *Astrophys. J.* 235:866–81
- Tohline JE. 1981. *Astrophys. J.* 248:717–26

- Tohline JE. 1982. *Fundam. Cosmic Phys.* 8:1–81
- Tohline JE. 1984. *Astrophys. J.* 285:721–28
- Tohline JE, Cazes JE, Cohl HS. 1999. *Numerical Astrophysics*, pp. 155–58. Boston: Kluwer
- Tohline JE, Durisen RH. 2001. See Zinnecker & Mathieu 2001, pp. 40–43
- Tohline JE, Durisen RH, McCollough M. 1985. *Astrophys. J.* 298:220–34
- Tohline JE, Hachisu I. 1990. *Astrophys. J.* 361:394–407
- Toman J, Imamura JN, Pickett BK, Durisen RH. 1998. *Astrophys. J.* 497:370–87
- Toomre A. 1964. *Astrophys. J.* 139:1217–38
- Truelove JK, Klein RI, McKee CF, Holliman JH II, Howell LH, Greenough JA. 1997. *Astrophys. J.* 489:L179–83
- Truelove JK, Klein RI, McKee CF, Holliman JH II, Howell LH, et al. 1998. *Astrophys. J.* 495:821–52
- Tsuribe T, Inutsuka S. 1999. *Astrophys. J. Lett.* 523:L155–58
- Tsuribe T, Inutsuka S. 2000. See Launhardt et al. 2000, pp. 184–86
- Valtonen M, Mikkola S. 1991. *Annu. Rev. Astron. Astrophys.* 29:9–29
- Vandervoort PO, Welty DE. 1981. *Astrophys. J.* 248:504–15
- Whitworth A. 1998. *MNRAS* 296:442–44
- Williams HA, Tohline JE. 1987. *Astrophys. J.* 315:594–601
- Williams HA, Tohline JE. 1988. *Astrophys. J.* 334:449–64
- Winkler K-H, Newman MJ. 1980. *Astrophys. J.* 236:201–11
- Wood D. 1982. *MNRAS* 199:331–43
- Woodward JW, Tohline JE, Hachisu I. 1994. *Astrophys. J.* 420:247–67
- Zinnecker H, Mathieu RD, eds. 2001. *The Formation of Binary Stars*. San Francisco: Astron. Soc. Pac.



## CONTENTS

---

FRONTISPIECE, <i>Edwin E. Salpeter</i>	xii
A GENERALIST LOOKS BACK, <i>Edwin E. Salpeter</i>	1
ULTRA-COMPACT HII REGIONS AND MASSIVE STAR FORMATION, <i>Ed Churchwell</i>	27
KUIPER BELT OBJECTS: RELICS FROM THE ACCRETION DISK OF THE SUN, <i>Jane X. Luu and David C. Jewitt</i>	63
THEORY OF GIANT PLANETS, <i>W. B. Hubbard, A. Burrows, and J. I. Lunine</i>	103
THEORIES OF GAMMA-RAY BURSTS, <i>P. Mészáros</i>	137
COSMIC MICROWAVE BACKGROUND ANISOTROPIES, <i>Wayne Hu and Scott Dodelson</i>	171
STELLAR RADIO ASTRONOMY: PROBING STELLAR ATMOSPHERES FROM PROTOSTARS TO GIANTS, <i>Manuel Güdel</i>	217
MODIFIED NEWTONIAN DYNAMICS AS AN ALTERNATIVE TO DARK MATTER, <i>Robert H. Sanders and Stacy S. McGaugh</i>	263
CLUSTER MAGNETIC FIELDS, <i>C. L. Carilli and G. B. Taylor</i>	319
THE ORIGIN OF BINARY STARS, <i>Joel E. Tohline</i>	349
RADIO EMISSION FROM SUPERNOVAE AND GAMMA-RAY BURSTERS, <i>Kurt W. Weiler, Nino Panagia, Marcos J. Montes, and Richard A. Sramek</i>	387
SHAPES AND SHAPING OF PLANETARY NEBULAE, <i>Bruce Balick and Adam Frank</i>	439
THE NEW GALAXY: SIGNATURES OF ITS FORMATION, <i>Ken Freeman and Joss Bland-Hawthorn</i>	487
THE EVOLUTION OF X-RAY CLUSTERS OF GALAXIES, <i>Piero Rosati, Stefano Borgani, and Colin Norman</i>	539
LYMAN-BREAK GALAXIES, <i>Mauro Giavalisco</i>	579
COSMOLOGY WITH THE SUNYAEV-ZEL'DOVICH EFFECT, <i>John E. Carlstrom, Gilbert P. Holder, and Erik D. Reese</i>	643

INDEXES

Subject Index	681
Cumulative Index of Contributing Authors, Volumes 29–40	709
Cumulative Index of Chapter Titles, Volumes 29–40	712

ERRATA

An online log of corrections to *Annual Review of Astronomy and Astrophysics* chapters (if any, 1997 to the present) may be found at <http://astro.annualreviews.org/errata.shtml>